Politecnico di Torino

Scuola di Dottorato

Dottorato in Meccatronica - XXIV Ciclo

Tesi di Dottorato

Design and Test of an Automotive Clutch Actuation

Autor

Michele Meloni

Supervisor

Andrea Tonoli

Febbraio 2012

Contents

Contents I

I Introduction 1

1 Introduction 3
- 1.1 Electro-Mechanical Actuators . . . 3
- 1.2 Linear EHS . . . 4
- 1.3 Linear Electro-Hydraulic Actuators . . . 5
- 1.4 Overview of the Technologies and Field of Study . . . 7
- 1.5 Thesis Aim . . . 8
- 1.6 Thesis Outline . . . 9

2 Bond graph 13
- 2.1 Brief Introduction on Bond graph . . . 13
- 2.2 Power Variables . . . 13
- 2.3 Bond Graph Element: 1-Port . . . 14
- 2.4 Element R . . . 15
- 2.5 Element C . . . 16
- 2.6 Element I . . . 16
- 2.7 Sources of Effort and Flow . . . 17
- 2.8 Junction Nodes . . . 18
- 2.9 Standard Elements: 2-Port elements . . . 19
  - 2.9.1 Transformer . . . 19
  - 2.9.2 Gyrator . . . 20
- 2.10 Causality Analysis . . . 20

II System Model and Improved Solution Design 23

3 Electro-Mechanical System 25

3.1 Introduction . . . 25
3.2 Gyrator: DC Motor . . . 26
3.3 Equivalent Inertia . . . 27
3.4 Transformators: Gearbox and Actuators . . . 27
3.5 Hydraulic Fluid . . . 28
3.6 Modeling Inertia and Load . . . 29
3.7 Bond Graph Scheme . . . 29
3.8 Equations of the System . . . 31
3.9 Non-linear load . . . 33

4 Model Validation **37**
4.1 Introduction . . . 37
4.2 Steady Gain Control . . . 37
4.3 Equivalent Mechanical Model . . . 38
4.4 Natural Frequencies: Bond-Graph and Mechanical Model . . . 39
4.5 Energy Analysis and Modal Displacements . . . 40
4.6 Experimental Data Validation . . . 42

5 Electro-Hydraulic Model **47**
5.1 Introduction . . . 47
5.2 Bondgraph Model and Equations . . . 47

6 Prototypes Design **53**
6.1 Present System . . . 53
6.2 Electromechanical with FISE Motor . . . 56
6.3 Electromechanical System: Maxon Motor and Gearbox . . . 61
6.4 Electro-Hydraulic System . . . 63
6.5 Mechanical Assembly . . . 67
6.6 CFD Analysis . . . 71

III Experimental test **75**

7 Experimental test and Results **77**
7.1 Electromechanical Systems . . . 79
7.1.1 Electromechanical System: FISE . . . 79
7.1.2 Electromechanical System: Maxon . . . 81
7.2 Electro-Hydraulic System . . . 83

8 Parameter Identification **87**
8.1 Non Linear Electromechanical Model . . . 87
8.2 Electric Motor and Gearbox . . . 87

8.3 Non Linear Cam 89
8.4 Hydraulic fluid and Clutch 90
8.5 Parameter Identification: EMA Systems 92
8.6 Parameter Identification: Electro-Hydraulic System 94

IV Conclusions **99**

9 Conclusions **101**

A Equations **1**
A.1 Mechanical Inertia Properties 1
A.2 Mechanic Equations 2
A.3 Hydraulic Equations 4
A.4 Non Linear EMA Model 6

Bibliography **A**

List of Figures **B**

List of Tables **G**

Part I

Introduction

Chapter 1

Introduction

Actuation systems were developed in aeronautics, manufacturing and robotic fields and the most arguments discussed to improve the performances were the different methods for modeling the control system and also the approaches of fail safe design. Generally can be used three different types:

- Electro-Mechanical Actuators, also called EMA;
- Hydraulic Systems:
  - Valve controlled circuits: also called EHS, Electro-Hydraulic servo valve actuators;
  - Hydrostatic trasmission circuits: also referred to EHA, Electro-Hydraulic Actuators.

In the following section a more detailed analysis is provided for each system, together with a state of the art review.

1.1 Electro-Mechanical Actuators

Electro-Mechanical Actuators could be used in automatic clutch actuators (see [10]) but were developed also in comparison to EHA system for aeronautic applications, in 2000 a EMA equipped F-18 flight-test [17]. The EMA solution consist in a brushed/brushless electric motor connected to a gearbox that could adapt the speed and torque of the system to the load and also transform motion from rotational to linear. It has a major advantage, it avoids oil contamination. This

kind of advantage, in automotive or aeronautic applications, is not a deal brake, but in food processing application could be a decisive factor.

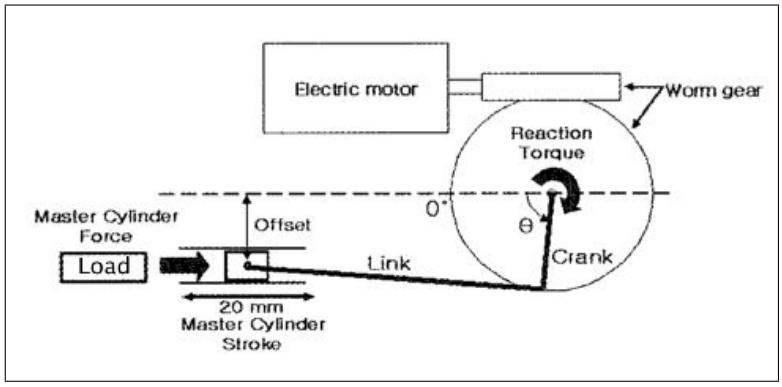

Figure 1.1. Electro-Mechanical system [10]

In figure 1.1 is shown a crank shaft mechanical system used to transform a rotation into a linear displacement. This system is far from efficient and it could be replaced for example with: a proper designed cam or a gear box and ball screw. In general high damping factors lead to a low performance system.

1.2 Linear EHS

EHS is still an important system for industrial applications; as for EHA systems these were developed with the evolution of fly-by-wire (FBW) technology to control flight surface actuation since 1970 [15] and [18]. These solution were developed using fixed displacement pump, Anderson [2] analyzed an EHA system with variable displacement pump.
The component that characterizes the system under consideration is the servo valve, which is controlled by the control unit to direct the flow to the actuator, be it linear (double-acting cylinder) or rotational (hydraulic motor with fixed or variable displacement). The flow is produced by a fixed displacement pump that is keyed on an induction motor.

This system, that is based upon the use of valves, got the weakness to produce pressure drop, and therefore power loss, when the valve is activated. This kind of actuation has five different designs 1.2:

1. Fixed displacement pump at constant supply pressure: this is the plant with lower efficiency with the relief valve put into the circuit for emergency reasons, the loss area is, indeed, huge;

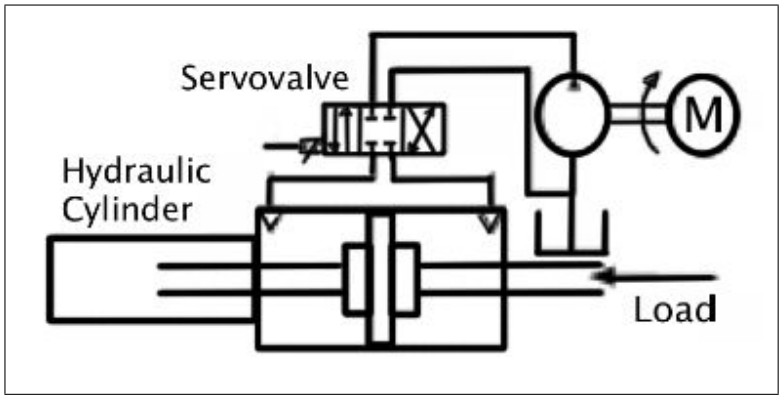

Figure 1.2. Generic EHS system

2. Fixed displacement pump pressure match: an load sensing circuit is added to the first system in order to have the pressure matching, loss area shrinks;
3. Pressure-compensated (could be fixed or variable) variable displacement pump: the pump is needed to provide a more efficient power source and it supplies fluid at flow rate matched to the system requirements;
4. Variable displacement pump power match (could be fixed or variable): in this kind of plant the only loss is due to the pressure drop in the directional valve, because the system is built using a variable displacement pump with power match;
5. Fixed displacement pump with bleed-off: the last design produces a flow excess, as the input pressure is matched totally to the pressure needed to actuate the load.

Taking into account the energy losses shown in figure 1.2, the fourth and fifth solutions are the most efficient. These plants are, indeed, compact and easy to control because there are less component that can introduce dynamics in the system.

1.3 Linear Electro-Hydraulic Actuators

In contrast to the configurations EHS is useful to consider the linear EHA (Electro-Hydraulic Actuators) solutions that are characterized by being constituted by a hydraulic cylinder connected to a pump in a closed circuit, without any servo valves. There is also an electric motor (brushless in general) that controls the hydraulic pump. You can have, moreover, two configurations:

- EHA-SM (Servo Motor) driven by a controlled brushless electric motor;
- EHA-SP (Servo Pump) driven by an induction motor and a brushless motor that is connected to a gearing to change the displacement of the pump.

The work of [11, 12] these system are analyzed in detail. In detail, [11] takes into account the EHA system from an industrial point of view after a deep analysis of the design methodology and validation. Instead [12] shows a deep review about the comparison between the EHA system and the EHA system.

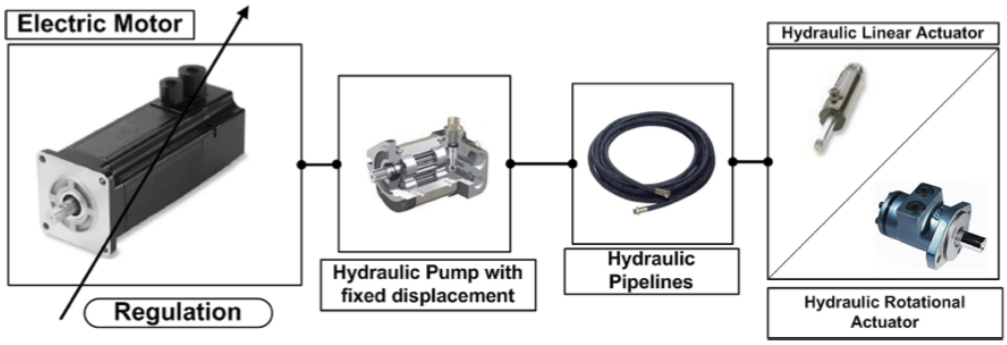

Figure 1.3. EHA system scheme, with principal components

The spread of high performance brushless motors, together with the inverters, makes them a very good option to have easily configurable system with excellent performances in terms of controllability.
The fixed displacement gear pumps are a good choice even if their volumetric efficiency decreases at low speed, but these pumps allow small size together with high speeds and high pressures. Closed hydraulic pipelines are used, moreover, to allow a highly configurable system. The absence of a tank involves the need to preload all the hydraulic circuit with a bias pressure, in order to prevent cavitation on the branch of low pressure, which can be each of the pipelines depending on the flow direction. The pre-charge pressure is ensured by an accumulator connected to the hydraulic pipelines through non-return valves, which are designed to make pass the fluid only in the direction from the accumulator to the circuit and block the reverse flow. Relief valves must be provided to protect the hydraulic components in case of excessive pressure. The closed circuit is devoid of a system for the heat exchange for the fluid, already present in the classic hydraulic circuits to the mere presence of a reservoir, therefore, for each individual application, it may be necessary to provide a heat exchanger, with the purpose of controlling the temperature of the fluid.

1.4 Overview of the Technologies and Field of Study

In this section the strong points of each system are analyzed to find the best possible technology in the present field.

- **Oil contamination**; EMA system are indeed the best solution if contamination is not an option;
- **Reliability and maintenance**: EHA-EHS could be rearranged to be safer than a EMA system, enabling the possibility to work even if a trouble-shoot occurs (patent), also having filter in the system leads to have less maintenance than a electromechanical system;
- **Packaging**: it is possible to mount a EHA-EHS system with more freedom, having a better flexibility over an EMA plant;
- **Power and volume density**: power to weight ratio on EHA-EHS system are 5 times bigger than that of the electromechanical system, moreover the power to volume ratio expected is 15-20 times bigger (see [17]);
- **Dynamic Behavior**.

In general hydraulic systems have the edge in most fields, but in order to choose the best solution it is important to consider the aim of the project . In [1, 18] works it is possible to find more detailed information about the differences and strong points of this technologies.
The aim of the thesis is to find the best solution, for a clutch actuation system, with high performance. Of course, it is useful to recall some solutions proposed to fulfill this task. First we can consider the solution adopted by Sila Holding, which is based on an electromechanical system. This configuration is rather complicated and cumbersome undoubtedly, also the opening times are high. The system is very similar to the solution presented by Moon and all. [10], differs only for the presence of an eccentric which replaces the connecting rod-crank mechanism.
In opposition to this solution we can consider the system developed by Magneti Marelli (see [9]) that can be identified as an EHS system. The latter, in fact, is characterized by implementing the clutch through a first proportional three-way two-position solenoid valve disposed upstream of a first set of two on-off solenoid valves, and a second proportional pressure solenoid valve disposed upstream of a second set of two on-off solenoid valves. Said valves are normally controlled by an electronic processing unit in accordance with the signals from sensors mounted on the vehicle and by the driver's controls. The pressurized fluid for driving the actuators is supplied by an electro-hydraulic power unit, that consists of a motor-driven

pump with a reservoir. An overpressure valve is provided for limiting excessively high pressure due to anomalous operation. That system has high performance but is characterized by a certain constructive complexity, for the presence of a large number of components.
A third option for the system is proposed in the patent [8], which describes a plant type EHS Bleed-Off used to implement a clutch and a method for calibration of the pressure sensor taking into account the depression produced by the pump. A bleed-off system, as seen previously (section 1.2), besides being efficient is also simple to build and control.
Also Honda motor patented a hydraulic clutch actuation [6], where an on-demand variable displacement pump and a purge valve connected between the pump and the piston are controlled by an electronically unit to provide the right pressure to the clutch actuator.
Such systems may have an improved performance by improving the control technology, this choice is widely used and an example can be found in the patent [16]. One goal of this work is to make the control less sensitive to the parameters of the vehicle on which it is used. More solutions were focused on the control: [4] considers the control of a pneumatic actuation system with particular attention at the travel comfort, instead, [3] work is about the control of a hydraulic plant.

1.5 Thesis Aim

From the previous sections, it's clear that the various systems used for the implementation over time have advantages and disadvantages, and that under certain conditions the choice may fall on one or the other solution. It then becomes necessary to define the scope in order to understand which path to take.
This thesis builds on the analysis of a automatic system for automotive automatic clutches. In this field of study there are some constraint to take into account and through them it is possible to find the best technological solution. As shown in previous sections the EHA systems were used in the past because they have high power to volume ratios, however, in recent times, they were replaced by electromechanical systems in order to avoid oil contamination. The system under consideration is characterized as electromechanical, electric motor brush DC, as well as a reduction system very complex.
The system was modeled using the Bond-Graph technique [5, 13, 14], treated in the chapter 2, which allowed the drafting of the dynamical system equations, in state space form. In fact the system itself is quite complex due to the fact that multiple dynamic domains were taken into account. The Bond-Graph technique was born, indeed, for the purpose to write equations about multi physics problems. The first

domain analyzed is electric (electric motor), then the mechanical properties of the motor, and gearbox are taken into account (inertia, damping factors, reduction ratios) and in the end the hydraulic fluid characteristic are modeled as fluid stiffness and viscous damping. The result is a unique model where all the dynamics are represented, with constitutive equations. The model was drafted with Lamberto Fusi's help [7]. These Matlab&Simulink equations, implemented through the analysis of the system, have allowed the identification of key parameters and design issues (see chapters). Starting from this situation, we proceeded to identify the main problems of the project, then alternative solutions have been proposed to improve performance and reduce power consumption and system complexity.

The solutions proposed are three:

1. Electromechanical system with reuse of the original engine with a gear ratio change and as a result of the inertia of the system;
2. Electro-mechanical system with new high efficiency motor and gearbox, high power system;
3. Electro-hydraulic system with high-performance design of the circuit routing and support of fluid valves.

The objective of the first two systems is to test the EMA system with minor changes and understand how these modifications can improve the performances. The hydraulic system, instead, aims to make the system much more compact and lightweight while maintaining or improving the performance level. In order to keep low complexity and high efficiency the EHS Bleed-Off configuration is chosen.

1.6 Thesis Outline

Chapter 1 describes the state of the art in EMA, EHS and EHA system and the evolution of such actuation with respect to the field of application. The chapter describes, moreover, the patents filled by companies which apply EHA and EHA systems in the transmissions field. It contains, also, the thesis objectives.
Chapter 2 provides a brief introduction on the Bond-Graph technique, the chapter explains the characteristics of the Bond-graph components and how to connect them in order to model the whole system.
Chapter 3 reports the characteristics of the SILA prototype and the modeling phase. All the equation are drafted and the final State Space model is defined.

Chapter 4 reports the numerical validation of the model and also the parameter identification to perform the experimental validation. In this phase the data collected from SILA were fundamental.
Chapter 5 describes the electro-hydraulic model and its equations.
Chapter 6 reports the prototypes design. In this chapter the most important steps taken are explained, components choice, design of the housing, safety concerns. In the first part the project key points are exploited and the electro mechanical solutions are described in detail; in the second part the hydraulic system is introduced.
Chapter 7 shows the results obtained during the experimental campaign conducted with the three prototypes. Also a description of the final test rig is proposed.
Chapter 8 demonstrates the identification procedure followed in order to find the unknown parameters of the model.
Chapter 9 reports the conclusions reached through experimentation and the comparison between the different solutions emphasizing the advantages and disadvantages of each.

System	Circuit application	Graphical representation	efficiency
Fixed displacement pump (1)	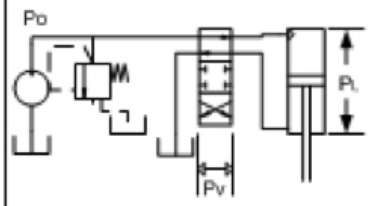	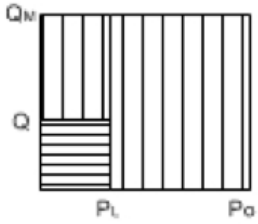	$\eta = \frac{P_l Q}{P_0 Q_M}$
Pressure Match (2)	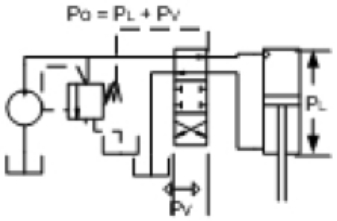	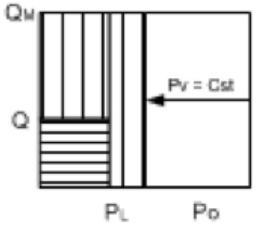	$\eta = \frac{Q/Q_M}{1+\frac{P_v}{P_l}}$
Pressure Compensated (3)	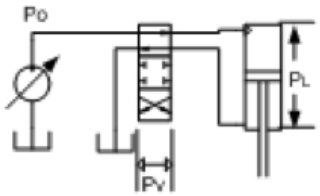	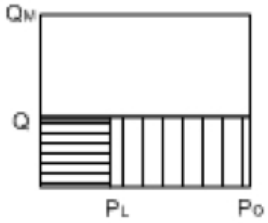	$\eta = \frac{P_l}{P_v}$
Power Match (4)	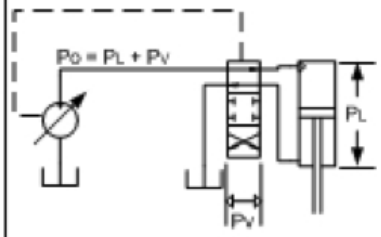	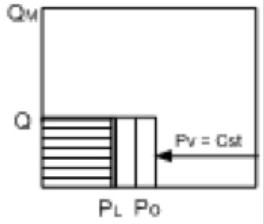	$\eta = \frac{1}{1+\frac{P_v}{P_l}}$
Bleed-off (5)	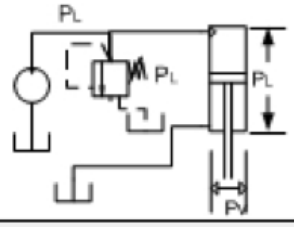	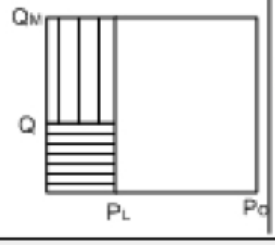	$\eta = \frac{Q}{Q_M}$

Figure 1.4. Energy losses in various EHS designs

Chapter 2

Bond graph

2.1 Brief Introduction on Bond graph

The Bond graph technique [5, 13] is a graphical tool that allows to observe the exchange of power within a physical system in order to analyze its behavior. In 1959 Prof H.M. Paynter had the revolutionary idea of graphically modeling a system in terms of power, connecting the elements of the physical system with appropriate joints and constraints. This depiction of the exchange of power was called Bond Graph. Bond Graph theory was improved by many researchers and extended to the modeling of hydraulic systems, mechatronics, electronics. This approach can represent a system using symbols and lines. Nowadays, from the graphic representation is possible to extrapolate the equations, in a systematic manner, through appropriate algorithms. A determining factor in the choice of technique Bond-Graph is that this technique allows the modeling of complex mechatronic systems, in which there are dynamic electrical, mechanical and hydraulic. In this chapter sections the main features of the Bond-Graph will be discussed in order to simplify the understanding of the mathematical models presented later.

2.2 Power Variables

The language of Bond Graph has the ambition to become a general method for describing interacting systems of power. The power exchange between the elements is defined using two variables: the Effort and Flow, which have different interpretations depending on the energy domain. The advantage of bond graph

consists in the possibility of building a single graphical representation of the system even if it consists of the interconnection of different energy domains. In table 2.1 shows the physical parameters considered **effort** and **flow**, depending on the energy domain.

Energy Domain	**P**	**Effort**	**Flow**
Linear Mechanics	$F \cdot v$	$F = dP/dt$	$v = dq/dt$
Rotational Mechanics	$T \cdot \omega$	$T = dP_\theta/dt$	$\omega = d\theta/dt$
Electric	$e \cdot i$	$e = d\lambda/dt$	$i = dQ/dt$
Hydraulic	$p \cdot Q$	$p = d?/dt$	$Q = dV/dt$
General	$e \cdot f$	$e = dP/dt$	$f = dq/dt$

Table 2.1. Effort and Flow in different energy domains

The power and always defined by the product of two quantities:

- Intensity or **e** (effort): voltage (e), force (F), torque (T), pressure (p)
- Flux or **f** (flow): current (i), linear speed (V), angular speed (ω), volume flow (Q)

So, in general, the power and calculated as:

$$P = e \cdot f \tag{2.1}$$

This is the basis for defining the language of the Bond-graphs (diagrams of bond). This principle and used by many computer codes based on block diagrams, such as "Sym-mechanics" or "Power system toolbox" in Matlab environment, where a single thread of connection determines a power exchange.

2.3 Bond Graph Element: 1-Port

The single port element is an element which is connected to the system with a single power exchange, within the Bond-graph theory it is represented by a single link. Four variables are the base of the system: effot (**e**), flow (**f**), the integral in time of the effort (**p**) and the integral in time of the flow (**q**).

Electrical domain: the physical components have two terminals (leads) that allow you to transfer electrical power.

- Resistance;

- Inductance;
- Capacity.

Mechanical domain:

- Mass and Inertia: the interface for the exchange of power is respectively point of contact force-torque-mass or inertia.
- Ideal Spring (mass not involved): the displacement difference between the extremes of the spring determines the force F generated and the work done.
- Ideal Damper (mass not involved): the same principle being presented for the ideal spring, but the strength is determined by the difference in speed between its extremes.

2.4 Element R

The resistor element is characterized by an equation that links statically the flow to the effort. Usually this element is used to represent a dissipation of energy:

- Damper (either linear or rotational) in mechanical domain;
- Resistor in electrical domain;
- Restriction in hydraulic domain.

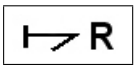

The half arrow element **R** represents an output produced by the incoming flow **f** and the effort **e**. In the constitutive relation, moreover, time does not appear explicitly, so the behavior is time-invariant. The **R** components is characterized by the absence of hysteresis and define a unique curve, on the chart **e** - **f**. The relationship between effort and flow is not necessarily linear.

$$e = R \cdot f \tag{2.2}$$

$$Power = e \cdot f = R \cdot f^2 \tag{2.3}$$

The component **R** is dissipative, the only way to regain the energy previously supplied to the component would go back in time.

2.5 Element C

The element **C** is a dynamic element which stores and transfers energy without any loss. The symbol that represents this element bond is **C**.

- Spring (either linear or rotational) in mechanical domain;
- Capacity in electrical domain;
- Accumulator in hydraulic domain.

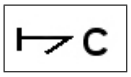

The **C** component represents a static relationship between the effort variable and the displacement **q**.

$$e = K \cdot q \tag{2.4}$$

$$q = \int_{-\infty}^{t} f \cdot dt \tag{2.5}$$

$$e = K \int_{-\infty}^{t} f \cdot dt \tag{2.6}$$

The component **C** is conservative since the energy involved is time-independent, but it is related only on the initial and final generalized displacement **q**.

2.6 Element I

This is the second element in single port that can store and give back energy in a bond graph, and it is called inertia.

- Mass and Inertia in mechanical domain;
- Inductor in electrical domain;
- No loss restriction in hydraulic domain.

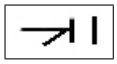

The characteristic equation links the momentum **p** with the flow **f** at any point in time

$$f = \frac{1}{J} \cdot p \tag{2.7}$$

$$p = \int_{-\infty}^{t} e \cdot dt \tag{2.8}$$

$$f = \frac{1}{J} \int_{-\infty}^{t} e \cdot dt \tag{2.9}$$

For these components there is a static relationship between the variables **f** and **P**, not necessarily linear (one example is the inductor when the ferromagnetic material is in a state of saturation), or intrinsically linear (masses that move at speeds far from speed of light). The component **I** is conservative, the energy depends only on the initial state and the final one. In fact, if a force is applied to a mass, it accelerates, vice versa if it brakes, the kinetic energy from the motion of **I** will be fully refunded, regardless of the time needed to accelerate the mass.

2.7 Sources of Effort and Flow

The ideal source of effort ($\mathbf{S}_e$) sets **e** independently of **f**. This is true in case of ideal components, instead real components will have a limited generated power; it means that beyond a certain amount of power, the constitutive relation will be no more valid. In the electrical domain is the ideal voltage. In the mechanic field there are not equivalent components, but an example may be the force of gravity which imposes a force regardless of the speed of the mass.
The only possible causality for these components is to impose the effort **e** over the system, the flow **f**, instead, will be defined by the system.
The flow source is the component dual of $\mathbf{S}_e$, since it imposes imposes a flow that is independent of the effort. The sources of effort are represented by the symbol $\mathbf{S}_e$, while $\mathbf{S}_f$ is used to symbolize that relating to the flow.

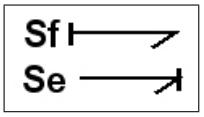

2.8 Junction Nodes

In the bond graph theory there are only two types of junctions: "**1**" and "**0**"; The combination of these joints with components identifies a physical system. In the case of a junction the characteristic equation is like:

The positive signs of the flows are defined by the arrows of the elements of the Bond-graph. In general, normal components will have incoming power, on the contrary, sources will have outgoing power. Even in the Bond-graph language, the junction can not accumulate nor dissipate energy, so all the energy/power will be managed by the components connected to the junction itself:

Junction Parallel (Zero)

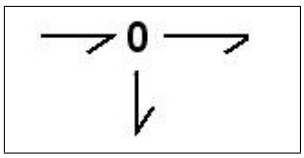

The sum of the flows in the node is equal to zero and the power input to the node will be equal to the output. In general, the powers involved depend only on the components connected to the node and the node (system analyzed at low frequencies to high frequencies may also have radiated energy).
e_i for each i-th component connected to the node is identical.

$$\sum \beta_j \cdot f_j = 0 \tag{2.10}$$

β_j takes the values "1" or "-1" depending on whether the outgoing and incoming power.

Junction Series (One)

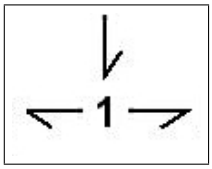

The sum of the efforts in the node is equal to zero. The flow in input is equal to the flow in output.
f_i for each i-th component connected to the node is identical.

$$\sum \beta_j \cdot e_j = 0 \tag{2.11}$$

β_j takes the values "1" or "-1" depending on whether the outgoing and incoming power.

2.9 Standard Elements: 2-Port elements

There are only two kinds of standard elements with two doors, called "Transformer" or "Gyrator". Within the Bond-Graph technique these symbols are represented by TF and GY, respectively, the transformer and the gyrator.

2.9.1 Transformer

The transformer element does not create or store energy. In general, the component **TF** connects entities of the same type between input and output, through its constitutive relation.

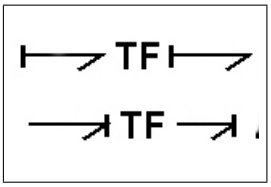

The equations relating the flow in the effort in input to those in output are represented by the following system:

$$\begin{cases} e_{in} = \tau \cdot e_{out} \\ f_{out} = \tau \cdot f_{in} \end{cases} \tag{2.12}$$

The input power is equal to the power in output:

$$P_{in} = e_{in} \cdot f_{in} \qquad P_{out} = e_{out} \cdot f_{out} \tag{2.13}$$

from (2.12) and (2.13) it is possible to write down (2.14):

$$P_{out} = \frac{1}{\tau} \cdot e_{in} \cdot \tau \cdot f_{in} \rightarrow P_{out} = e_{in} \cdot f_{in} = P_{in} \tag{2.14}$$

Examples of this kind of component:

- Gearbox or Lever in mechanical domain;
- Electrical transformer;
- Linear actuator or pump in hydraulic domain.

2.9.2 Gyrator

In Bond-Graph the gyrator element is represented by **GY**. This element makes a link between flows and efforts using constant values.

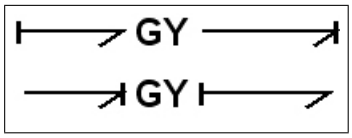

As in the case of the transformer, the gyrator does not store energy.

$$\begin{cases} e_{in} = K \cdot f_{out} \\ e_{out} = K \cdot f_{in} \end{cases} \tag{2.15}$$

$$P_{in} = e_{in} \cdot f_{in} \qquad P_{out} = e_{out} \cdot f_{out} \tag{2.16}$$

from (2.16) and from (**??**) it could be found (2.17):

$$P_{out} = K \cdot f_{in} \cdot \frac{1}{K} \cdot e_{in} \rightarrow P_{out} = e_{in} \cdot f_{in} = P_{in} \tag{2.17}$$

2.10 Causality Analysis

Having defined the characteristics of the system in terms of components 1 or 2 ports, and connections, you must define the causality imposed by them, to understand the input and output variables.

1. Identify mandatory causalities (Sources).
2. Consider the propagation of causalities depending on the characteristics of nodes in which the components are connected. For example, in the case of a generator, when connected to a node 0, the causalities on the other components are defined.
3. Where, however, it is not possible to propagate the causality, it is necessary to impose additional causality (i.e. the presence of states) to conservative components, one at a time, spreading the causalities imposed up to where it is possible. For example if there is an inductive component on which impose the causality. By doing so it will force the flow on node on which it is connected. This will be propagated by the node to the other components.

At this point, having defined the components that make up the system and having them connected by appropriate joints, it is possible to write down the equations of the states. These result from the node equations and equations defined characteristics of the components having the proper causality of the same.

Part II

System Model and Improved Solution Design

Chapter 3

Electro-Mechanical System

3.1 Introduction

Sila Holding Industriale is an Italian company with 1800 employes all over the world: Italy, Brasil, India etc. Its core business is automotive gearbox components, but it has a R&D department based in Italy that proposes and develops innovative systems. One of the ideas was to develop a robotized gearbox with an Electro-Mechanical actuation.
This implementation consists of three blocks, electrical, mechanical and hydraulic, the first is composed by a DC motor with brushes, the output shaft of the electric motor is bound to the mechanical system which consists of a reduction and a eccentric. The cam is driven by the reduction and it moves a piston, called master, the hydraulic fluid is compressed in such a way as to allow the movement of the hydraulic piston (slave), mechanically connected to the clutch lever. The aim of the company was to have the prototype analyzed (see figure 3.1) and to find some clues to improve it.
The goal of the project was to evaluate this prototype, to find any weakness and improve its performances. In the following sections every part is analyzed and modeled using Bond-Graph techniques. The resulting model is used, therefore in order to discover the issues of the design and to produce an improved system.
The following sections describe the various parts of the model and introduce the equations that rule the system dynamics.

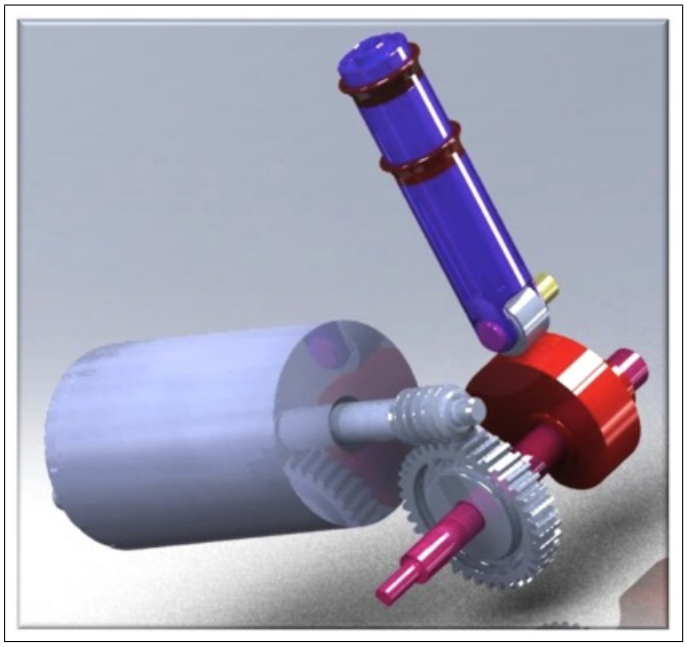

Figure 3.1. Prototype SILA Holding Industriale

3.2 Gyrator: DC Motor

The electric motor used by SILA Holding Industriale is a DC brush motor which is controlled in position. We can, therefore, assume that the motor has a current input, it is therefore possible to neglect the electrical dynamics in the characteristic equations.

$$\begin{cases} T = K \cdot I \\ E = K \cdot \omega \end{cases} \tag{3.1}$$

Where **T** is the torque generated by the electric motor, **I** the current flowing in the motor, **E** the electromotive force and ω is the angular velocity of the rotor; the constant **K** is a matter of the motor used.
As described in the chapter 2 the torque **T** and the electromotive force **E** are considered to be **efforts**, while the current **I** and speed ω are **flows**. Among the basic Bond-Graph elements this component, can be modeled with the gyrator, that binds the flow to the effort and vice versa.

$$\begin{cases} e_{in} = K \cdot f_{out} \\ e_{out} = K \cdot f_{in} \end{cases} \tag{3.2}$$

3.3 Equivalent Inertia

The mechanical properties of the electric motor, left out in the first part of this chapter, are modeled along with those of the reduction system in this section.
The first step was to take into account the inertial components with respect to the rotor speed, multiplying the inertial value to the correspondent reduction ratio. If the shafts are considered infinitely rigid connection, only one of the inertia component connected via a gearbox can be a state of the system, the other, therefore, depend on it. The gearbox is made up of a worm wheel which drives a second gear in PVC that is tied to the output shaft and the eccentric. The ratio between the worm wheel and gear output is equal to 38:1 (τ). This value is used to write the following equations, where J_{in} is a total inertial equivalent, for a more detailed explanation see appendix A.1.

$$J_{in} = J_{DCmotor} + J_{Wheel} + \frac{1}{\tau} \cdot (J_{Gearbox} + J_{Shaft} + J_{Cam}) \tag{3.3}$$

3.4 Transformators: Gearbox and Actuators

Actuators and gearboxes are dedicated to the transformation of effort and flow without altering the power, in particular the actuators are responsible for changing the energy domain. The SILA Holding solution is to use two linear actuators with cylindrical chamber section but with slight different values of diameter, and their task consists in generating a hydraulic power from mechanical one and vice versa. It identifies itself as the master actuator which generates a hydraulic pressure operated by the eccentric, while the slave receives the pressure generated by the master and operate the clutch lever. In the Bond Graph model two **TF** elements (trasformators) are used to model the actuators and gearbox. The first **TF** is directly related to the eccentric, and it turns the linear speed of the cam in a hydraulic flow, while the latter turns the hydraulic flow in linear velocity. The input-output relationship of the transformation is (3.4)

$$\begin{cases} f_{out} = K \cdot f_{in} \\ e_{in} = K \cdot e_{out} \end{cases} \tag{3.4}$$

Master Actuator

$$\begin{cases} e_{in} = [N] \\ f_{in} = \left[\frac{m}{s}\right] \\ e_{out} = \left[\frac{N}{m^2}\right] \\ f_{out} = \left[\frac{m^3}{s}\right] \end{cases} \quad \rightarrow \quad K = [m^2] \tag{3.5}$$

Slave Actuator

$$\begin{cases} e_{in} = \left[\frac{N}{m^2}\right] \\ f_{in} = \left[\frac{m^3}{s}\right] \\ e_{out} = [N] \\ f_{out} = \left[\frac{m}{s}\right] \end{cases} \quad \rightarrow \quad K = \left[\frac{1}{m^2}\right] \tag{3.6}$$

3.5 Hydraulic Fluid

The hydraulic fluid is modeled under the hypothesis that there is air dissolved in the circuit, as it implies a deformability dynamic change. The circuit is equipped with a system to evacuate the air, so the above assumptions can be taken. The fluid in the system introduces two physical effects: energy storage and power loss. The compressibility of the fluid is considered as a **C** component which stores and releases energy. The power dissipation due to viscosity of the fluid is represented as a **R** component. In the hydraulic bond graph is modeled as in Figure 3.2.

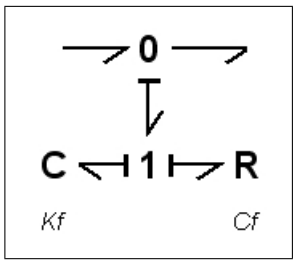

Figure 3.2. Hydraulic system model

The node **0** shown in 3.2, is used to introduce fluid model in the system. A variation of the fluid volume δV causes a pressure change δP.

$$\Delta P = K_f \cdot \Delta V \tag{3.7}$$

$$e = K_f \cdot \int_0^t p \, dt \tag{3.8}$$

Since the difference in volume is the integral of the compressibility of the hydraulic fluid flow, it is modeled as an element **C** which has the stiffness value K_f. K_f is proportional to the oil bulk modulus β_{fluid} and inversely proportional to the total volume V_{line} of the hydraulic circuit.

$$K_f = \frac{\beta_{fluid}}{V_{line}} = \frac{\beta_{fluid}}{l_{line} \cdot A_{line}} \tag{3.9}$$

Where A_{line} represents the section of water pipes and l_{line} is the length of the pipes. The damping effect is modeled considering a reduction in pressure, related proportionally to the change in hydraulic flow.

$$\delta P_c\,(t) = C_f \cdot \delta Q\,(t) \tag{3.10}$$

Looking at the equation (3.10), the coefficient C_f is meant to be a **R** component, because it multiplies a volume flow rate.

3.6 Modeling Inertia and Load

The slave actuator, driven by hydraulic fluid, and the clutch lever share the same speed. From the Bond Graph point of view this means that they are connected by a series node (1). The weight of the thrust bearing can be modeled with an item **I**. The slave actuator load modeling can not be done with a single port element, as its characteristic 3.3 is highly non-linear. To obtain a dynamic similar to the real load, the non linear spring is approximated by a linear one (item **C**) and a source of effort: the aim of the source of effort is to correct the force generated by the linear spring in order to obtain the desired force.

3.7 Bond Graph Scheme

Once you have identified the components, the Bond-Graph technique is used to model the system through the table 3.1. The first step, before proceeding to the construction of the table, is to identify the flow and the effort shared among the

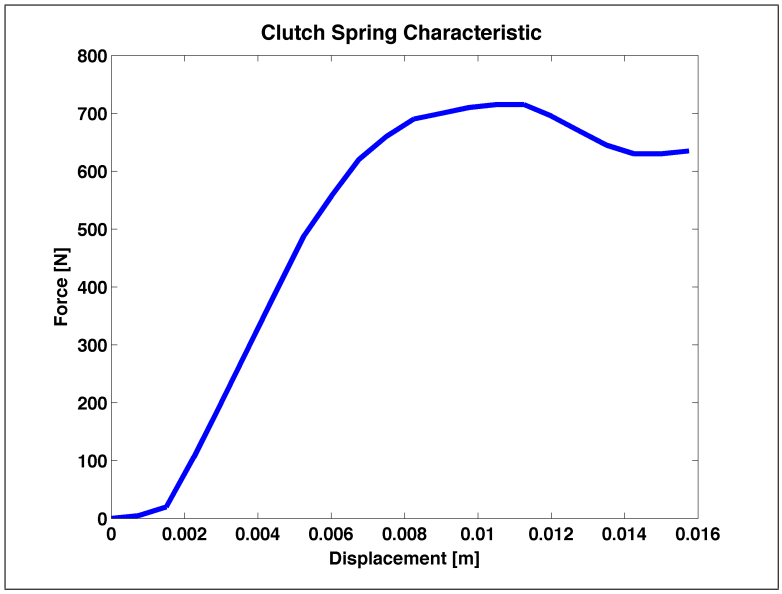

Figure 3.3. Characteristic load Slave Actuator

components; secondly, the common variables over the junction nodes **1** and **0** have to be defined. The resulting Bond-Graph scheme is shown in Figure 3.4

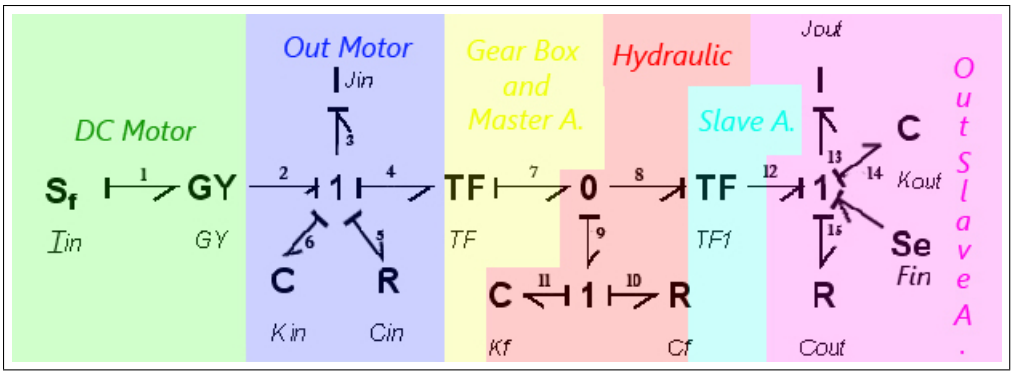

Figure 3.4. BondGraph Scheme of the original sistem.

The engine is represented as a source of **flow** connected to a gyrator, it is connected to the remaining part of the Bond-Graph through a node **1**, the flow over this node is the angular velocity of the motor rotor. The inertia, friction and stiffness are rotating at the same angular speed of the electric motor.
The angular speed is transformed, then, by the cam in a linear speed with an a **TF**. This is given as an input to the fluid system, and transformed again, through another **TF** in linear speed to actuate the clutch spring. Here, to model the non linear load, as explained in section 3.6, there are a linear spring (**C**) and an source

of effort $\mathbf{S}_e$. These are connected to a **1** node together with an inertial component **I** (the mass of the thrust bearing) and **R** component that deals with the piston viscous friction.

3.8 Equations of the System

The Bond graph method greatly simplifies the procedure for the preparation of the equations system, in particular the procedure to arrive to a model variable state becomes almost systematic. It begins with the construction of a table which shows all the characteristic equations of the individual components

N.	Component	IN	OUT	Equation
1	Sf	e_1	f_1	$f_1 = I_{in}$
1-2	GY			$e_2 = K \cdot f_1 \; f_2 = K \cdot e_1$
3	I	e_3	f_3	$e_3 = \dot{p_3} \; f_3 = 1/J_{in} \cdot p_3$
5	R	f_5	e_5	$e_5 = R \cdot f_5$
4-7	TF			$e_4 = \tau \cdot e_7 \; f_7 = \tau \cdot f_4$
8-12	TF			$e_8 = \tau \cdot e_{12} \; f_{12} = \tau \cdot f_8$
10	R	f_{10}	e_{10}	$e_{10} = R \cdot f_1 0$
11	C	f_{11}	e_{11}	$f_{11} = \dot{q_{11}} \; e_{11} = K_f \cdot q_{11}$
13	I	e_{13}	f_{13}	$e_{13} = \dot{p_{13}} \; f_{13} = 1/J_{out} \cdot p_{13}$
14	C	f_{14}	e_{14}	$f_{14} = \dot{q_{14}} \; e_{14} = K_{out} \cdot q_{14}$
15	R	f_{15}	e_{15}	$e_{15} = R \cdot f_{15}$
A	**1**			$f_2 = f_3 = f_4 = f_5 \; e_2 = e_3 + e_4 + e_5$
B	**0**			$e_7 = e_8 = e_9 \; f_7 = f_8 + f_9$
C	**1**			$f_9 = f_{11} = f_{10} \; e_9 = e_{10} + e_{11}$
D	**1**			$f_{12} = f_{13} = f_{14} = f_{15} = f_{16} \; e_{12} + e_{16} = e_{13} + e_{14} + e_{15}$

Table 3.1. Collection of the characteristic equation of the original system with Bond-Graph

Through the states identified in table 3.1 it is possible to get the matrices [**A**], [**B**], [**C**] and [**D**]. These are the four matrices that describe the dynamic model by means of input variables, states and obviously outputs.
The following equations represent the four states that describe the system dynamics, in appendix A.2 is presented the equations drafting:

$$\dot{p_3} = K_i I_{in} - \frac{C_{in} + C_f \tau_1^2}{J_{in}} p_3 - \frac{K_f}{\tau} q_{11} + \frac{\tau_1 C_f}{\tau_2 J_{out}} p_{13} \tag{3.11}$$

$$\dot{q_{11}} = \frac{\tau_1}{J_{in}} p_3 - \frac{1}{\tau_2 J_{out}} p_{13} \tag{3.12}$$

$$\dot{p_{13}} = \frac{\tau_1 C_f}{\tau_2 Jin} p_3 + \tau_1 K_f q_{11} - \frac{\left(C_{out} + \frac{C_f}{\tau_2^2}\right)}{J_{out}} p_{13} - Koutq_{14} + F_{in} \tag{3.13}$$

$$\dot{q_{14}} = \frac{1}{J_{out}} p_{13} \tag{3.14}$$

Matrices
From (A.11),(A.13),(A.18),(A.20) it is possible to obtain the state vectors:

$$\mathbf{x} = \begin{Bmatrix} p_3 \\ q_{11} \\ p_{13} \\ q_{14} \end{Bmatrix} \tag{3.15}$$

then the dynamic matrix **A** and the matrix of inputs **B** are written:

$$\mathbf{A} = \begin{bmatrix} -\frac{C_{in}+\frac{C_f}{\tau^2}}{J_{in}} & \frac{K_f}{\tau} & -\frac{\tau_1}{J_o ut} & 0 \\ \frac{1}{J_{in}} & 0 & 0 & 0 \\ \frac{1}{\tau J_{in}} & 0 & \frac{\tau_1}{J_{out}} & 0 \\ \frac{\tau_1 C_f}{\tau Jin} & \tau_1 K_f & -\frac{C_{out}+\tau_1^2 C_f}{J_{out}} & -K_{out} \\ 0 & 0 & \frac{1}{J_{out}} & 0 \end{bmatrix} \tag{3.16}$$

$$\mathbf{B} = \begin{bmatrix} K_i & 0 & 0 & 0 \\ 0 & 0 & 1 & 0 \end{bmatrix} \tag{3.17}$$

A system state variables is characterized by a system like this:

$$\begin{cases} \{\dot{x}\} = [\mathbf{A}]\{x\} + [\mathbf{B}]\{u\} \\ \{y\} = [\mathbf{C}]\{x\} + [\mathbf{D}]\{u\} \end{cases} \tag{3.18}$$

To complete the system modeling the matrix **C** and the matrix **D** have to be found; this is only possible after identifying the outputs of the system. The following variables have to be known in order to identify the system response:

1. Motor Speed;
2. Slave Actuator Speed;

3. Slave Actuator Force.

The speed of the electric motor is identified from the **flow** f_3 which is subject to the state p_3

$$f_3 = \frac{1}{J_{in}} p_3 \tag{3.19}$$

With regard to the slave actuator speed, this coincides with the f_{13}

$$f_{13} = \frac{1}{J_{out}} p_{13} \tag{3.20}$$

The spring of the clutch is defined from **effort** e_{14} therefore on the table 3.1

$$e_{14} = K_{out} q_{14} \tag{3.21}$$

at this point from equations (3.19), (3.20), (3.21) it is possible to write down **C** e **D**

$$\mathbf{C} = \begin{bmatrix} 0 & 0 & \frac{1}{J_{out}} & 0 \\ \frac{1}{J_{in}} & 0 & 0 & 0 \\ 0 & 0 & 0 & K_{out} \end{bmatrix} \tag{3.22}$$

$$\mathbf{D} = \begin{bmatrix} 0 & 0 \\ 0 & 0 \\ 0 & 0 \end{bmatrix} \tag{3.23}$$

3.9 Non-linear load

In the previous paragraph it has been said that the load, which is non-linear, is modeled using Bond-Graph with a linear spring and a source of strength. In this section we analyze how the correction is made to obtain the desired characteristic. As seen in figure 3.4 the characteristic slave force/displacement is identified by an element **C** connected to the node **1**, which identifies the slave actuator speed. This node is connected, also, to a source of effort S_e, this does not exist in the physical system; the source consists in correcting the linear force component **C** in order to obtain the characteristic shown in Figure 3.3.

$$e_{12} + e_{16} = e_{13} + e_{14} + e_{15} \tag{3.24}$$

where e_{16} is the effort generated by the source (see image 3.6) and e_{14} is the linear spring force (image 3.5):

$$e_{12} = e_{14} - e_{16} + e_{13} + e_{15} \tag{3.25}$$

With this technique, the junction **1** receives the non-linear load (3.3) as a difference: $e_{14} - e_{16} = F_{slave}$.

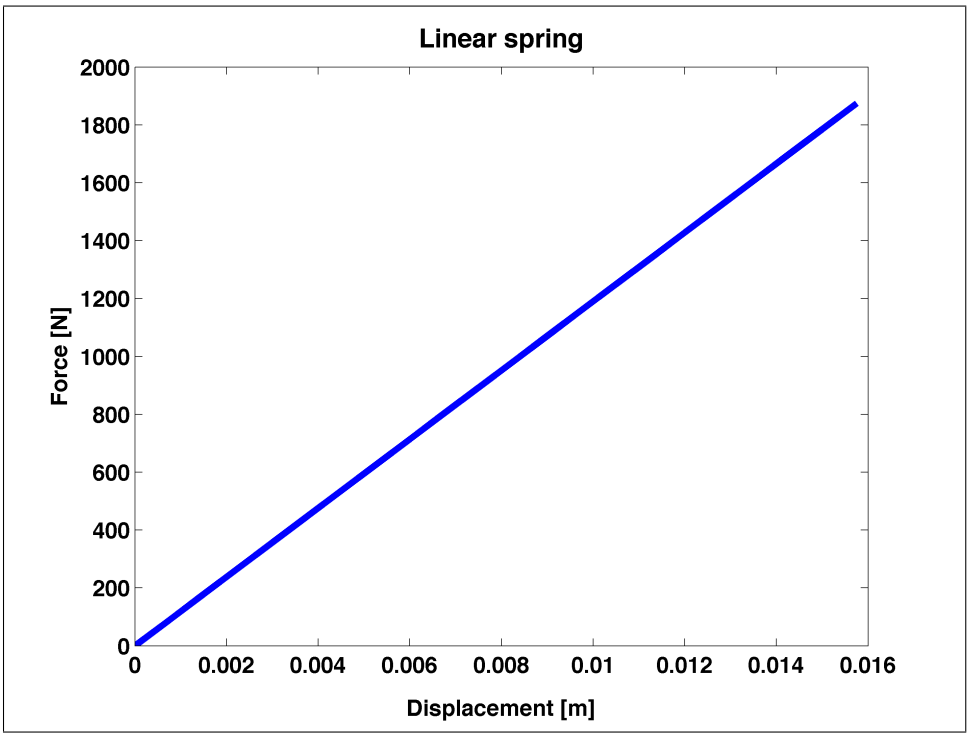

Figure 3.5. Slave load modeling, linear feature

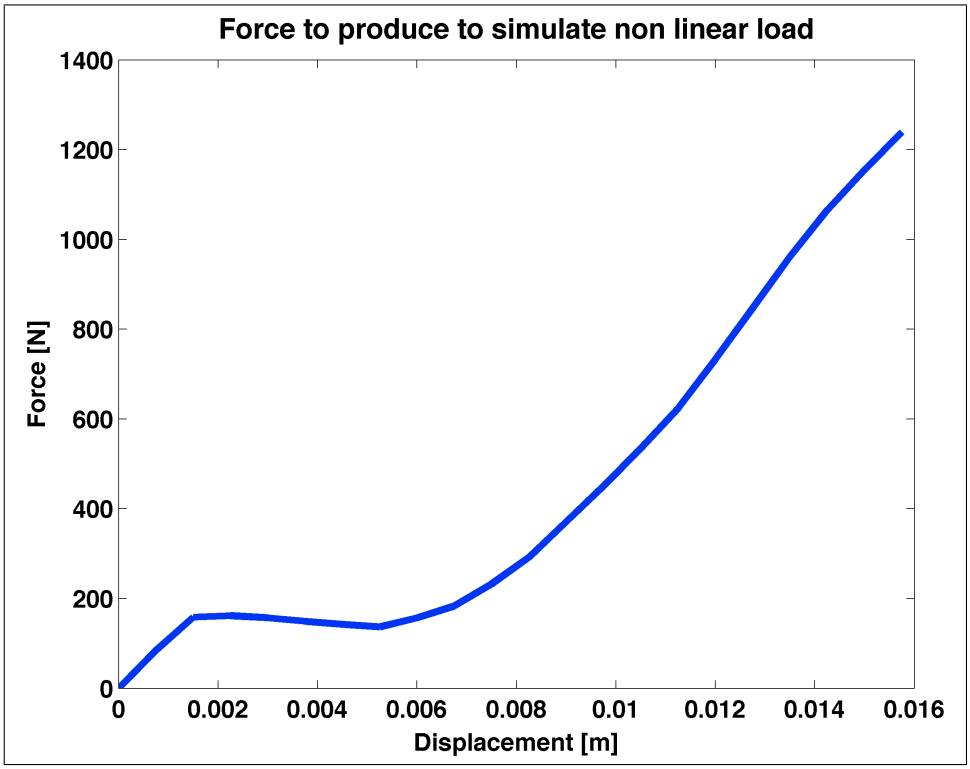

Figure 3.6. S_e characteristic

Chapter 4

Model Validation

4.1 Introduction

The construction of a mathematical model is not only writing down the dynamic equations, but, above all, it is to verify that the resulting model reflects reality as closely as possible.
To do so the unknown parameters must be found or guessed, in order to match the experimental data with the numerical ones.
Various techniques could be used to find the aforementioned parameters, some of those were used during the characterization process and they will be explained in the present chapter.

4.2 Steady Gain Control

The first step taken to verify that the model represents the SILA holding system was to check that the overall ratio between input and output was correct. The transfer function between the torque of the motor and the slave actuator force is shown in figure 4.2, the stationary gain is equal to the overall ratio: $9.33 \cdot 10^3$ (79.4 [dB]).
The overall ratio calculated with the convention [in]/[out] is equal to $9.35 \cdot 10^3$.

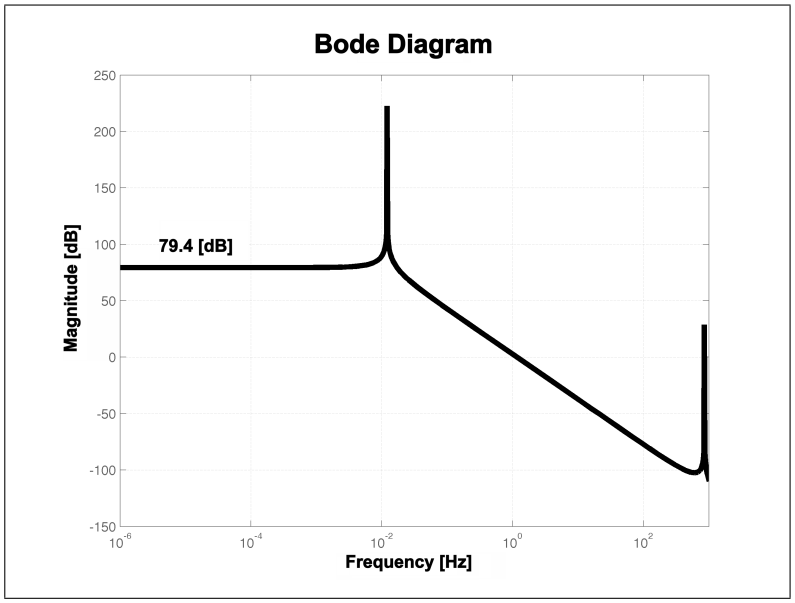

Figure 4.1. Frequency response of the system (Damping neglected)

4.3 Equivalent Mechanical Model

A feasible choice is to only two inertial elements, to simplify the model: one that represent the input inertia and it combines Motor, Gearbox and Cam, this solution leaves the thrust bearing as second mass of the system. These two masses are connected using elements with a determined stiffness. If we neglect damping elements, the scheme shown in Figure 4.2 is the equivalent mechanical system.

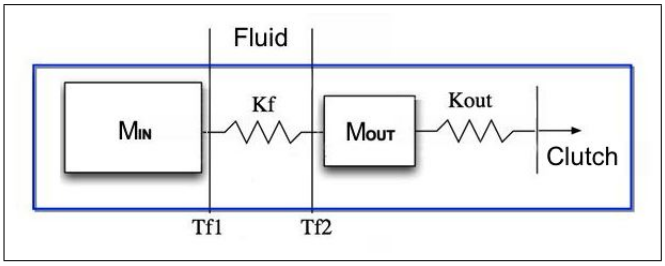

Figure 4.2. Mechanical equivalent of the original system

The inertia input is transformed into a mass by dividing the value for the total ratio squared (4.1).

$$M_{in} = \frac{J_{in}}{\tau^2} \tag{4.1}$$

The stiffness of the fluid is multiplied by the square of the area of the slave actuator, to obtain its mechanical equivalent.

$$K_{f_{eq}} = K_f \cdot A_{slave}^2 \tag{4.2}$$

Parameter	Unit	Value
M_{in}	[kg]	$5.37 \cdot 10^3$
K_f	$[\frac{N}{m}]$	$8.57 \cdot 10^6$
M_{out}	[kg]	$3 \cdot 10^{-1}$
K_{OUT}	$[\frac{N}{m}]$	$1.2 \cdot 10^5$

Table 4.1. Equivalent model parameters

4.4 Natural Frequencies: Bond-Graph and Mechanical Model

From figure 4.2, the mechanical equivalent is a 2 DOF system, this means that it has two modes of vibration at two distinct frequencies.
The pulsation that characterizes the oscillation is given by (4.3):

$$\omega = \sqrt{\frac{K_{out}}{M_{in} + M_{out}}} \tag{4.3}$$

To calculate the pulsation see eq. (4.4):

$$\omega = \sqrt{\frac{K_f + K_{out}}{M_{out}}} \tag{4.4}$$

The values obtained using this approach have to be compared to those obtained using the Bond-Graph model. To obtain the natural frequencies of the model (the damping factor is neglected) an analysis of the eigenvalues of **A** is performed.

Table 4.2 shows that the natural frequencies are close.

	Mechanical Model	Bond Graph Model
Mode 1 [Hz]	0.75	0.744
Mode 2 [Hz]	856	856

Table 4.2. Comparison of natural frequencies of the two models

4.5 Energy Analysis and Modal Displacements

In the previous section are described modes of vibration of the mechanical equivalent model and the frequencies at which the oscillations occur, a further verification of the model is to analyze where the energy is concentrated within the system. Within the system there are two elements which can store elastic potential energy **E**, while the two masses possess their own kinetic energy **U** (see (4.5)).

$$U = \frac{1}{2}K\left|x\right|^2 \qquad E = \frac{1}{2}J\left|v\right|^2 \tag{4.5}$$

The eigenvectors λ of the matrix **A** correspond to the movements of the modal state variables; these are momentums and displacements. If the momentums is divided for its speed the masses are obtained, at this point it is possible to calculate the energies associated with each element. From the geometric theory this 2 DOF system has four modal states or eigenvalues (v), therefore the eigenvector matrix must be λ_{4x4}:

$$Av \;=\; \lambda v \tag{4.6}$$

Both the kinetic energy that the potential were then normalized with respect to the total energy of the system related to every eigenvalue.

$$\begin{aligned} E_{tot_{fn}} &= \tfrac{1}{2}J_{in}\left|v_{in_{fn}}\right|^2 + \tfrac{1}{2}J_{out}\left|v_{out_{fn}}\right|^2 \\ U_{tot_{fn}} &= \tfrac{1}{2}K_{in}\left|x_{in_{fn}}\right|^2 + \tfrac{1}{2}K_{out}\left|x_{out_{fn}}\right|^2 \end{aligned} \tag{4.7}$$

v and x are the eigenvectors representing the speed and the displacement, respectively, with respect to the masses and stiffness of the system for every eigenvalue. The final step is shown in eq. (4.8) and it represents the normalization of the energy component.

$$\begin{aligned} E_{M_{in}} &= \frac{\frac{1}{2}M_{in}}{E_{tot_{fn}}} \cdot 100 \quad E_{M_{out}} = \frac{\frac{1}{2}M_{out}}{E_{tot_{fn}}} \cdot 100 \\ U_{K_f} &= \frac{\frac{1}{2}K_f}{U_{tot_{fn}}} \cdot 100 \quad E_{K_{out}} = \frac{\frac{1}{2}K_{out}}{U_{tot_{fn}}} \cdot 100 \end{aligned} \tag{4.8}$$

The same calculations are repeated for both frequencies with the following results:

	M_{in}	M_{out}
Frequence 1 (0.7Hz)	99.9946%	0.0054%
Frequence 2 (856Hz)	0.0054%	99.9946%

Table 4.3. Kinectic energies

Table 4.3 shows that at the frequency 2, the kinetic energy is almost entirely concentrated on the mass of the clutch thrust, while the inertia of the motor and gearbox has little energy, while the frequency 1 most of the energy kinetic energy is contained in the vibration of the inertia on the crankshaft, but this does not mean that the mass of the thrust bearing does not move. To analyze the latter condition is observed normalized eigenvectors, since the frequencies are complex conjugate eigenvectors 4 will be 4, but identical two by two, so we consider only 2.

	J_{in}	J_{out}
Frequence 1 (0.7Hz)	1	1
Frequence 2 (856Hz)	$3.4 \cdot 10^{-}4$	1

Table 4.4. Modal displacements normalized to the maximum in line

The table 4.4 points out how the first natural frequency of the masses are moving in the same way, only the value of the kinetic energy can be misleading because of the mass equivalent of J_{in} and J_{out}, there are four orders of magnitude of difference.
In table 4.5, for the first mode, it is to see how much of the potential energy is stored by the output spring (K_{out}). This is due to the fact that the two inertia move, as if they are rigidly connected, on the spring of the clutch. The second order, however, can be represented with the equivalent mass M_{in} fixed and the mass M_{out} that oscillates between springs K_f and K_{out}.

	K_f	K_{out}
Frequence 1 (0.7Hz)	1.36%	98.63%
Frequence 2 (856Hz)	98.63%	1.36%

Table 4.5. Potential Energies

4.6 Experimental Data Validation

In the previous sections of this chapter, the model was validated using eigenvalues and eigenvectors and with the frequency response analysis. In order to further refine the mathematical model a parameters identification has to be performed. To do so Simulink is used (see figure 4.6), this is a graphic tool to deploy the system starting from the model state variables.

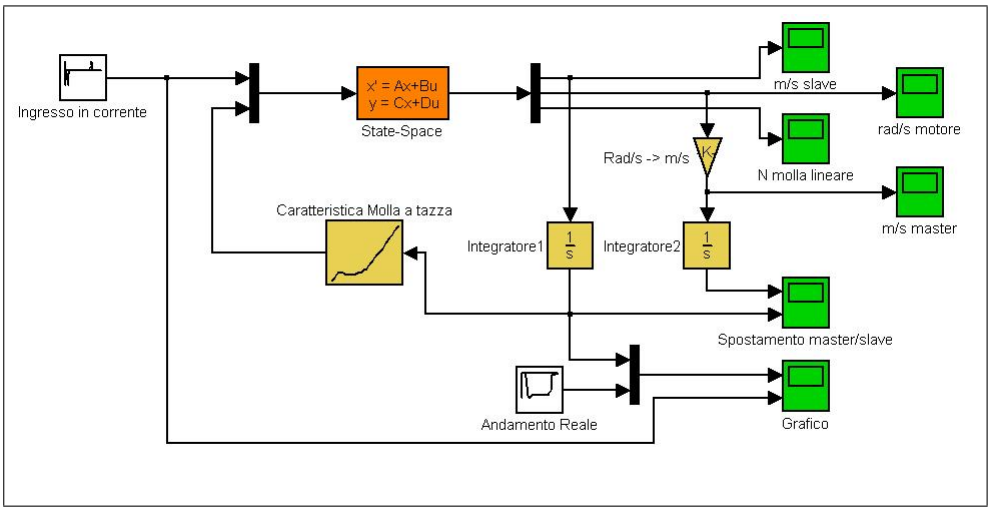

Figure 4.3. Simulink diagram used for simulation

The mathematical model is contained in a single block which requires the matrix [**A**], [**B**], [**C**], [**D**]. The inputs and outputs of the block **state-space** are created automatically based on the size of the matrix [**B**], [**C**], [**D**]; especially writing the matrix [**B**] and [**D**] the inputs of the system are needed, while the matrix [**C**] dimension is defined choosing how many outputs are useful to fully understand the system behavior.
The nonlinearity of the spring is created by an appropriate Simulink blocks that have the task of generating a force that corrects the characteristic of linear spring (see section 3.9) The correction of the load should vary depending on the deformation of the linear spring, this deformation corresponds to the actuator slave

displacement. The look-up table in figure takes as input the displacement of the slave and it gives in output the clutch load. The outputs of the **State-Space** are speeds and forces, to obtain the displacement of the actuator is enough to integrate in time its linear velocity. This parameter is fundamental, in fact it is used to compare the numerical value from the model with the experimental performance. In figure 4.6 there are many **Scope** elements, they have the task to store temporal trends of physical quantities of interest.

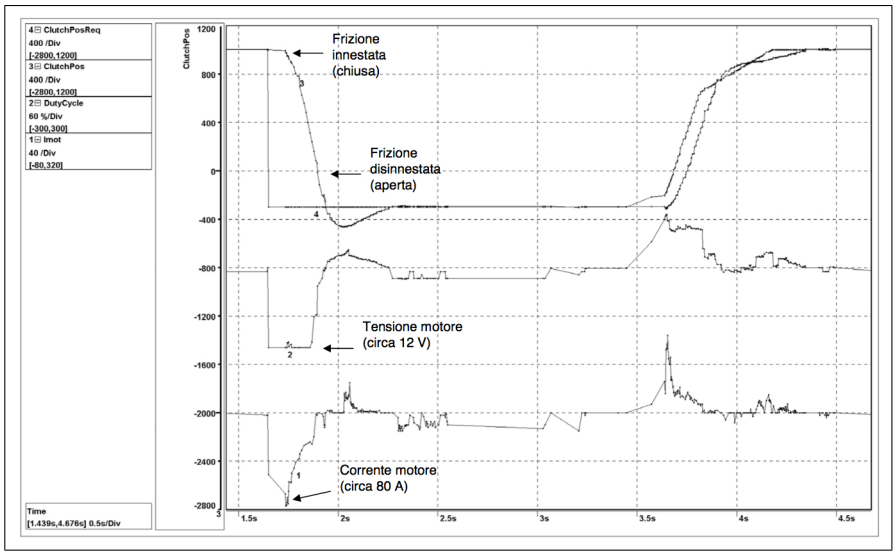

Figure 4.4. Current trends and positions provided by SILA Holding Industriale

The mathematical model takes into account the power dissipation by friction, such as the hydraulic fluid viscous friction and the friction of the master and slave cylinders. The values of these parameters, however, are not known and the target of the analysis is to approximate the behavior of the numerical model to that of the real system shown in figure 4.4. The first simulation, which does not take into account the unknown friction (eccentric reducer and contact-actuator master), was the first attempt, the result is shown in figure 4.5:

From figure 4.5 the behavior of the model, in red, it differs greatly from that of the real system in black. This is due to the fact that the mathematical model receives an input current signal (blue one on the bottom graph) similar to the current actually provided to the existing system. The reason why the slave actuator displacement in the numerical system is so big is due to the fact that the torque produced by the electric motor is more than enough to overcome the resistant force. The latter is smaller than the real one that could be described by the following equation (4.9) that describes a 1 DOF equivalent system.

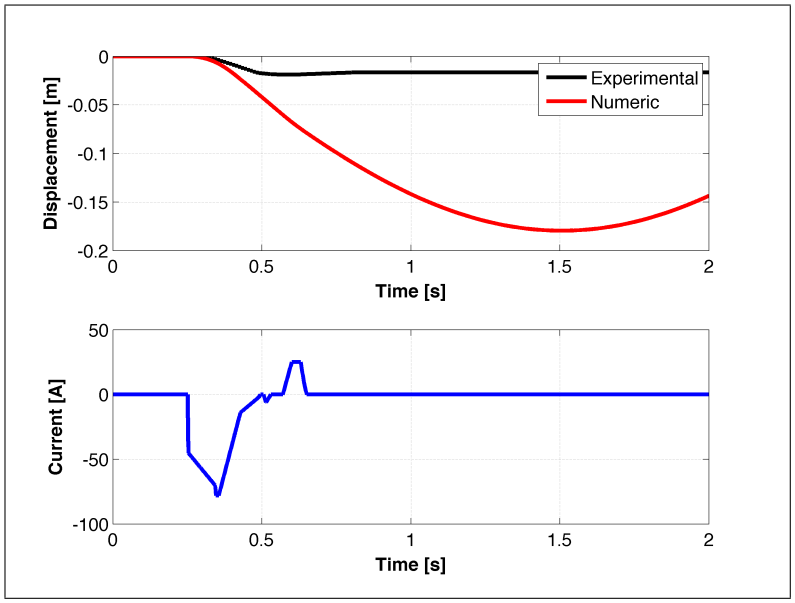

Figure 4.5. Top:Evolution in time of the slave displacement, all the damping parameters are equal to zero; Bottom: input current of the system

$$m\ddot{x} + c\dot{x} + kx = F_{tot} \tag{4.9}$$

From (4.9) the second term is equal to zero, when damping is neglected, so the displacement x with the same F_{tot} has to be bigger. One solution may be to consider the viscous friction of the piston master, but the difference from the case without friction is minimal. The simulation are not yet comparable with experimental data. In order to identify the correct value of friction, various simulations are performed. In a empirical way, by gradually increasing the value of viscous friction on the engine, the result obtained is an attenuation of the actuator slave displacement.

In figure 4.6 the displacement is consistent with the experimental data, even if the model takes too long to accelerate, this is probably due to a too high input inertia. Since the inertia of the gearbox and the eccentric were obtained by importing CAD drawings into SolidWorks, there might be some importation error or some mistake during the inertia calculation. To obtain the correct value of inertia the total input inertia has to be decreased of about 25% with respect to the theoretical value. The result is shown in 4.7

Having carried out the model validation, the model itself was used for dynamical simulations in order to design the high performance system, choosing the best solutions on market.

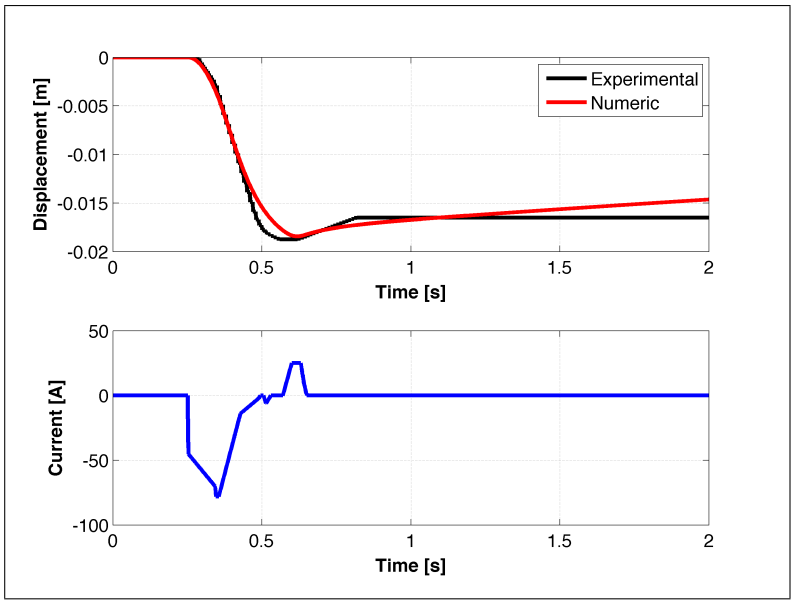

Figure 4.6. Top: Evolution in time of the slave displacement; Bottom: input current of the system

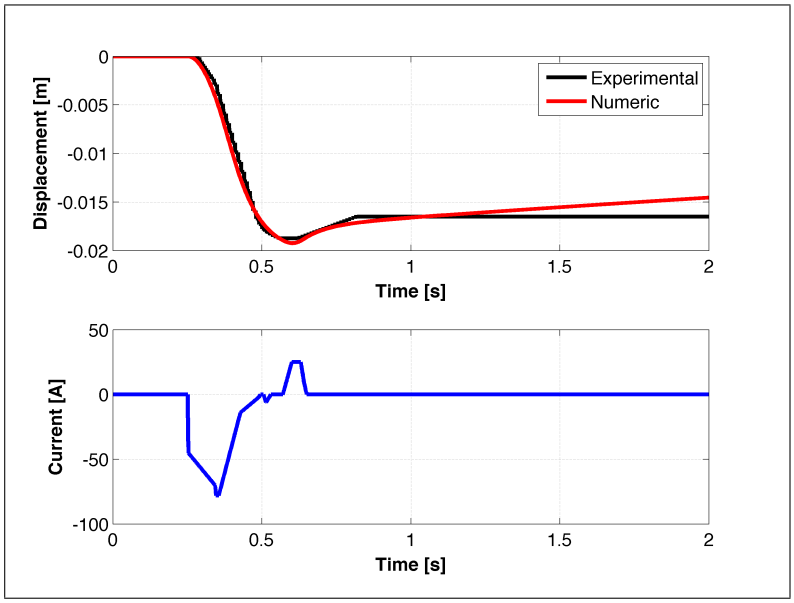

Figure 4.7. Top: Evolution in time of the slave displacement, identified system; Bottom: input current of the system

Chapter 5

Electro-Hydraulic Model

5.1 Introduction

The model of the hydraulic system is quite similar to the electromechanical one, this is due to the fact that they share some parts:

- Electric Motor;
- Fluid system;
- Clutch spring, bearing.

The difference is due to the presence of a hydraulic pump that substitutes the master cylinder and the gearbox. The pump is modeled using a **TF** element.
The system itself, as said in chapter 1 has the goal to be an high performance actuator with great power to weight ratio. To do so, the whole system consist of more components, like a relief valve to take into account safety issues and a electro-valve used to ensure the irreversibility of the system.
The hydraulic scheme and the mechanical one are shown in figures 5.1 and 5.2.

5.2 Bondgraph Model and Equations

The modeling procedure starts from the electric motor which introduces a source of **flow** connected to a gyrator, the input current is converted into torque, while the voltage is converted in speed. The output of the gyrator represents the mechanical part of the engine, so here it is connected a node **1**, which represents the speed of rotation. The overall inertia in input (permanent magnet rotor inertia plus pump

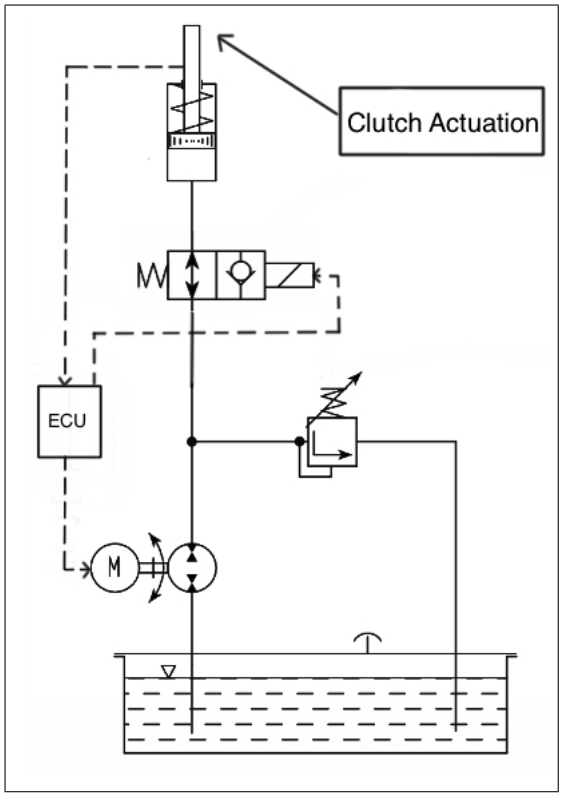

Figure 5.1. hydraulic scheme of the system

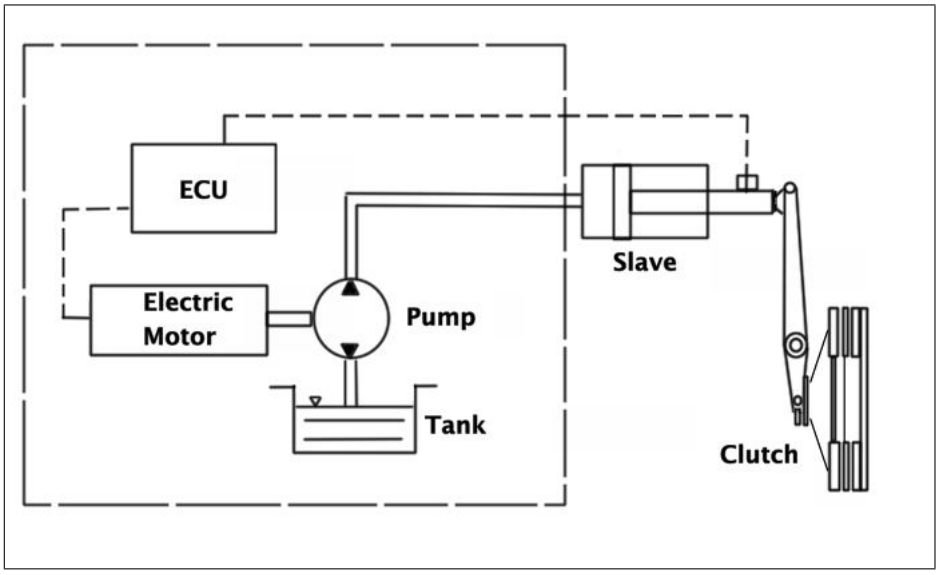

Figure 5.2. Mechanical Scheme of the electro-hydraulic system

inertia) and the friction, that has to be identified during experimental stages, are related to the speed of rotation, then these are to be connected with the gyrator **GY**. This modeling is equivalent to that performed for the electromechanical system, reference is made, therefore, to the procedure reported in chapter 3. The hydraulic pump introduces a change of physical domain, the item **TF** (τ equals the displacement of the pump) that identifies the mechanical part is interposed between the engine and the hydraulic fluid. The slave actuator, also, has the task of changing the domain then it was inserted a **TF** after the modeling of the fluid. The output of the **TF** is connected to a node **1** which represents the linear velocity of the actuator. The inertia of the thrust bearing and the load characteristic of the actuator are connected to the last **TF**. The pattern resulting bond graph is as follows:

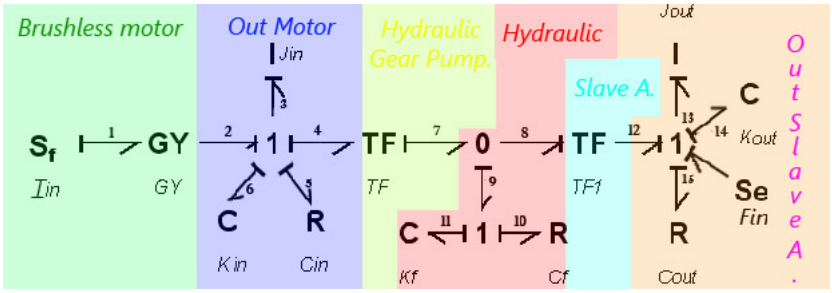

Figure 5.3. Bond Graph Scheme of the electro-hydrostatic system

Once the scheme is defined and the various nodes are identified, it is possible to write down the equations related to each component, for readability it was decided to put them on a table.

n°	Component	IN	OUT	Equation
1	Sf	e_1	f_1	$f_1 = I_{in}$
1-2	GY			$e_2 = K \cdot f_1 \; f_2 = K \cdot e_1$
3	I	e_3	f_3	$e_3 = \dot{p_3} \; f_3 = 1/J_{in} \cdot p_3$
5	R	f_5	e_5	$e_5 = R \cdot f_5$
4-7	TF			$e_4 = \tau_1 \cdot e_7 \; f_7 = \tau_1 \cdot f_4$
8-12	TF			$e_8 = \tau_2 \cdot e_{12} \; f_{12} = \tau_2 \cdot f_8$
10	R	f_{10}	e_{10}	$e_{10} = R \cdot f_10$
11	C	f_{11}	e_{11}	$f_{11} = \dot{q_{11}} \; e_{11} = K_f \cdot q_{11}$
13	I	e_{13}	f_{13}	$e_{13} = \dot{p_{13}} \; f_{13} = 1/J_{out} \cdot p_{13}$
14	C	f_{14}	e_{14}	$f_{14} = \dot{q_{14}} \; e_{14} = K_{out} \cdot q_{14}$
15	R	f_{15}	e_{15}	$e_{15} = R \cdot f_{15}$
A	**1**			$f_2 = f_3 = f_4 = f_5 \; e_2 = e_3 + e_4 + e_5$
B	**0**			$e_7 = e_8 = e_9 \; f_7 = f_8 + f_9$
C	**1**			$f_9 = f_{11} = f_{10} \; e_9 = e_{10} + e_{11}$
D	**1**			$f_{12} = f_{13} = f_{14} = f_{15} = f_{16} \; e_{12} + e_{16} = e_{13} + e_{14} + e_{15}$

Table 5.1. Equation of the bondgraph system

From Table 5.1 it has to identify those equations that contain a derivative, since these equations contains information on system states. The result is a model in state variables:

$$\{\dot{x}\} = [A] \cdot \{x\} + [B] \cdot \{u\} \tag{5.1}$$

As for the electromechanical model also for the hydraulic model the state equations are needed to build the A, B, C and D matrices. In appendix A.3 a detailed equation drafting can be found.

$$\dot{p_3} = K_i I_{in} - \frac{C_{in} + C_f \tau_1^2}{J_{in}} p_3 - \frac{K_f}{\tau} q_{11} + \frac{\tau_1 C_f}{\tau_2 J_{out}} p_{13} \tag{5.2}$$

$$\dot{q_{11}} = \frac{\tau_1}{J_{in}} p_3 - \frac{1}{\tau_2 J_{out}} p_{13} \tag{5.3}$$

$$\dot{p_{13}} = \frac{\tau_1 C_f}{\tau_2 Jin} p_3 + \tau_1 K_f q_{11} - \frac{\left(C_{out} + \frac{C_f}{\tau_2^2}\right)}{J_{out}} p_{13} - Koutq_{14} + F_{in} \tag{5.4}$$

$$\dot{q_{14}} = \frac{1}{J_{out}} p_{13} \tag{5.5}$$

From equations (A.26),(A.28),(A.33),(A.35) it is possible to obtain this state vector.

$$\mathbf{x} = \begin{Bmatrix} p_3 \\ q_{11} \\ p_{13} \\ q_{14} \end{Bmatrix} \tag{5.6}$$

Then it is possible to write the dynamic matrix **A** and the matrix of inputs **B**.

$$\mathbf{A} = \begin{bmatrix} -\frac{C_{in}+\frac{C_f}{\tau^2}}{J_{in}} & \frac{K_f}{\tau} & -\frac{\tau_1}{J_o ut} & 0 \\ \frac{1}{J_{in}} & 0 & 0 & 0 \\ \frac{1}{\tau J_{in}} & 0 & \frac{\tau_1}{J_{out}} & 0 \\ \frac{\tau_1 C_f}{\tau Jin} & \tau_1 K_f & -\frac{C_{out}+\tau_1^2 C_f}{J_{out}} & -K_{out} \\ 0 & 0 & \frac{1}{J_{out}} & 0 \end{bmatrix} \tag{5.7}$$

$$\mathbf{B} = \begin{bmatrix} K_i & 0 & 0 & 0 \\ 0 & 0 & 1 & 0 \end{bmatrix} \tag{5.8}$$

A system state variables is characterized by a set of equation like the following:

$$\begin{cases} \{\dot{x}\} = [\mathbf{A}]\{x\} + [B]\{u\} \\ \{y\} = [\mathbf{C}]\{x\} + [D]\{u\} \end{cases} \tag{5.9}$$

must still write the matrix **C** and the matrix **D**, this is only possible after identifying the outputs of the system. As you come out of the same system we described in earlier in this chapter:

1. Motor Speed;
2. Slave Actuator Speed;
3. Clutch Spring Force.

The speed of the electric motor is identified by the flow f_3 which is related to the state p_3

$$f_3 = \frac{1}{J_{in}} p_3 \tag{5.10}$$

With regard to the slave actuator speed, it is the f_{13}

$$f_{13} = \frac{1}{J_{out}} p_{13} \tag{5.11}$$

The force of the spring clutch is identified by the effort e_{14} and then from the table 5.1 it can be obtained,

$$e_{14} = K_{out} q_{14} \tag{5.12}$$

at this point using the equations (5.10),(5.11),(5.12) it is easy to write the matrices **C** e **D**.

$$\mathbf{C} = \begin{bmatrix} 0 & 0 & \frac{1}{J_{out}} & 0 \\ \frac{1}{J_{in}} & 0 & 0 & 0 \\ 0 & 0 & 0 & K_{out} \end{bmatrix} \tag{5.13}$$

$$\mathbf{D} = \begin{bmatrix} 0 & 0 \\ 0 & 0 \\ 0 & 0 \end{bmatrix} \tag{5.14}$$

The resulting model, implemented in Matlab&Simulink will be used to choose the components to build the prototype actuator.

Chapter 6

Prototypes Design

6.1 Present System

In order to understand the design procedure, it is fundamental to clarify the weaknesses of the prototype produced by FISE. In fact the design of the improved prototypes started from the present system and its construction (in figure 6.1):

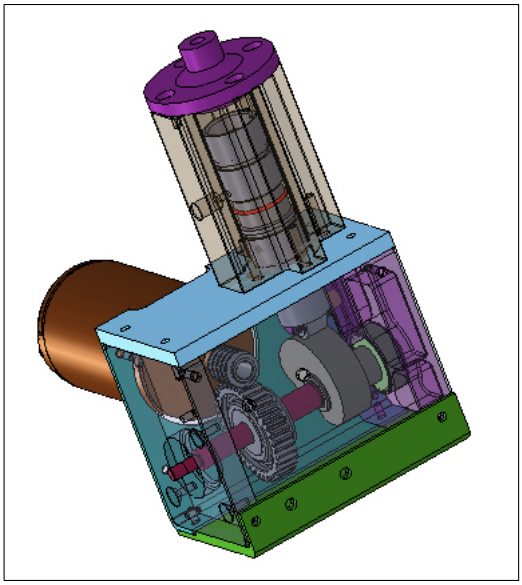

Figure 6.1. Present System from SILA Holding

The mathematical model described in chapter 3 was used to analyze the current system and understand what might be the problems that limited its performance. The analysis shows that the system present weaknesses both from the mechanical point of view and from the electrical point of view. First, with regard to the electrical domain, the low efficiency of the electric motor FISE ($\eta = 50\%$) is undoubtedly a determinant limiting factor. Moreover, this electric motor has some problems also from the mechanical point of view, a high inertia, solved through the choice of a new system. A possible solution is to use a new electric motor, more performant, linked to a new reduction system (see section 6.3). The SILA Holding Industrial has required, for cost containment, to foresee the re-use of the system FISE, in order to do this it was verified that another major problem of the system was the high transmission ratio due to the screw-nut system and worm wheel. The configuration with the re-use of the FISE motor will be described in detail in section (6.2).
The reduction system certainly has some problems. In the first place it is characterized by having a very high reduction value of 1/38, this value was determined at the SILA Holding to ensure non-reversibility of the system. This condition allows to maintain in a position to disengage the clutch without providing torque through the electric motor, using the internal friction of the gearbox. The non-reversibility of the system was not considered essential during the design of the improved system, it is preferred to focus on performances improving. In addition, a more efficient system allows to use less energy to maintain the clutch opened. Consequently both the high-performance system is the system with re-use of the motor FISE have benefited from the use of a planetary reduction systems, which are characterized by a high efficiency also because the reduction ratios were reduced.
Furthermore, as regards the mechanical systems we proceeded to some workings on the cam to be able to accommodate the shaft of the reduction gears and the bearing, this component was machined also to reduce its rotational inertia. The new solution is shown in figure 6.3 and it's the same for the two electromechanical systems. The inertia is 25 % lower than the original cam.

	Cam	**Cam Modified**
Inertia $[kgm^2]$	$4.82\,10^{-}5$	$3.49\,10^{-5}$

Table 6.1. Cam Inertia (Computed using Solidworks®)

On completion of the introduction of electromechanical systems, we introduce the solution electro-hydraulic, which is characterized in the replacement of the system for reducing mechanical system with a hydraulic pump as well as a set of components such as valves for the control and safety, and a hydraulic circuit. This system

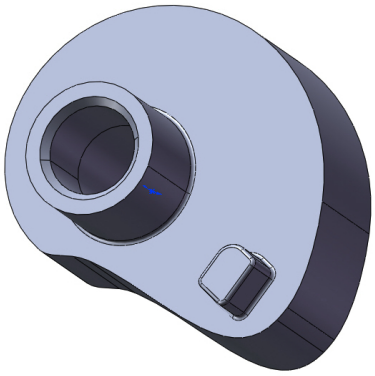

Figure 6.2. Cam

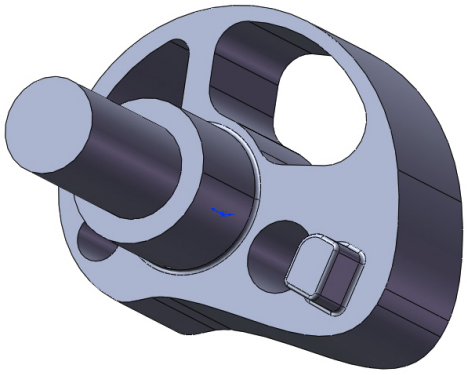

Figure 6.3. Modified Cam, with lower Inertia

is presented in detail in section 6.4. The three solution are the following:

1. Electromechanical solution with the FISE electric motor;

2. Electromechanical solution with high performances;

3. Electro-hydraulic solution.

The design of the systems listed above follows a few key points that were agreed with the company Sila Holding. First the improved system must be lighter and smaller that the previous version, during the market analysis to find electric motors and gearbox the weight of the components had to be taken into account. Also the material of housing structures was in mainly aluminum. The clutch actuator, moreover, must be mounted into the engine room where the available volume is minimal. Particular attention has been paid to the compact design of containment structures and the choice of components with high power to volume ratios.
Having designed three prototypes during the test campaign, in order to optimize the comparison between the systems, it will be necessary to establish a common test rig to which connect the various models. Also, to avoid dead times it was thought to favor the ease of assembly and disassembly. Therefore decomposable supports, with easy access, were produced for the electromechanical solutions.

6.2 Electromechanical with FISE Motor

The first solution was to use the FISE electric motor working together with a new planetary gearbox. The choice of the reduction system, as mentioned above, is based on the efficiency and the reduction ratio. As regards efficiency, the choice is definitely focuses on the planetary gears (see 6.4). Epicyclic gearing or planetary gearing is a gear system consisting of one or more outer gears, or planet gears, revolving about a central, or sun gear.

Figure 6.4. Planetary gearbox example

Advantages of planetary gears over parallel axis gears include high power density, large reduction in a small volume, multiple kinematic combinations, pure torsional reactions, and coaxial shafting. Disadvantages include high bearing loads, inaccessibility, and design complexity. The planetary gearbox arrangement is an engineering design that offers many advantages over traditional gearbox arrangements. One advantage is its unique combination of both compactness and outstanding power transmission efficiencies. A typical efficiency loss in a planetary gearbox arrangement is only 3% per stage. This type of efficiency ensures that a high proportion of the energy being input is transmitted through the gearbox, rather than being wasted on mechanical losses inside the gearbox. Another advantage of the planetary gearbox arrangement is load distribution. Because the load being transmitted is shared between multiple planets, torque capability is greatly increased. The more planets in the system, the greater load ability and the higher the torque density. The planetary gearbox arrangement also creates greater stability due to the even distribution of mass and increased rotational stiffness.
As regards the reduction ratio we have investigated the relationship between total engine torque input and the force acting on the slave cylinder. The minimum reduction value capable of ensuring the opening of the clutch has been identified in 1/11. A reduced τ can also reduce the size of the system. The τ final value is defined by the products on the market, the system more similar to that ideal one

is produced by the MAXON company: GP 42 (see 6.5). In the table the main characteristic of the motor and the gearbox are shown 6.2.

	Electric Motor	**Gearbox**
Name	FISE Brushed Motor	Planetary Gearhead GP42C
Speed [rpm]	500	8000[1]
Max Torque[Nm]	12	4.5
η_{MAX} [%]	52.1	90
Weight [g]	1000	260

Table 6.2. Motor and Gearbox Characteristics

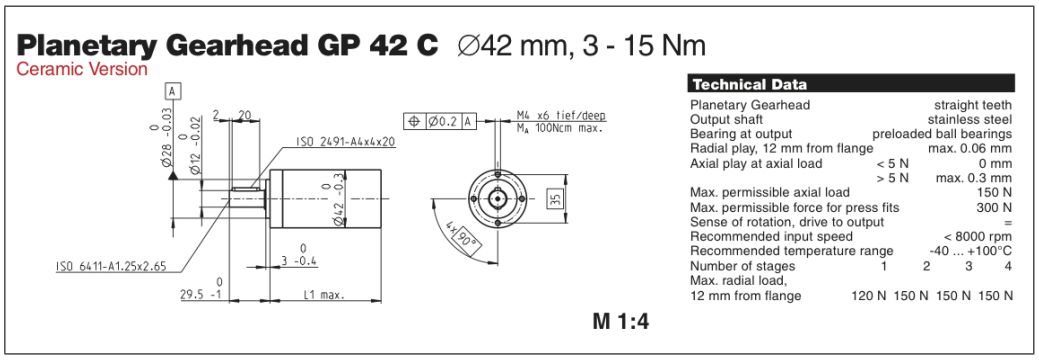

Figure 6.5. Key components

The characteristics of the selected gear have been used to simulate the behavior of the system through the Simulink model. The results obtained are shown in the figure and show how this configuration allows to obtain improved performance 6.6.

The components of the new system are now defined, at this point the final part is about designing an housing structure. This structure should preferably have the following characteristics:

- **Compact**
- **Easy assembly**: in order to achieve this objective the mechanical component is composed by four parts mounted together using screws;
- **Capable to accomodate different system versions**: this is explained in the related section (see section 6.2);

[1]Max speed allowed

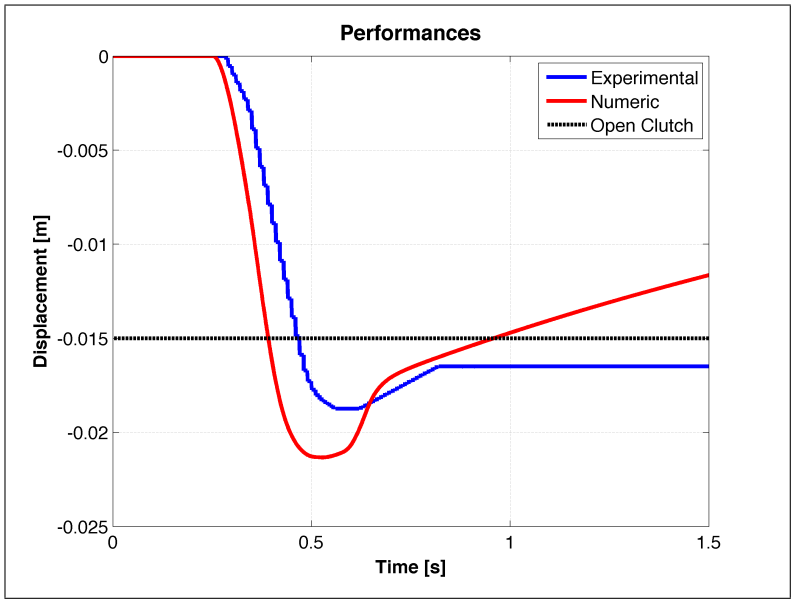

Figure 6.6. Numerical simulation of the system with FISE motor and Maxon gearbox ($\tau = 1/12$); Opening time: 140 [ms]

- **High precision assembly**: centering pins are used to achieve a axial precision near 10 [μm] (see section 6.2);
- **Modularity**: this structure can be used with little differences by the two electromechanical systems.

In order to have a compact system, the design of the housing started from an aluminum billet. The first solution is shown in figure 6.7. The component had to connect, with maximum precision, the system parts; this choice is due to the fact that one important issue was to achieve collinearity of the gearbox, the cam and the bearing. From an experimental point of view, however, is more advantageous to have a prototype easy to assemble and disassemble. Consequently it was decided to break down the original component into four parts (as shown in figure 6.8), which are connected with each other through a series of screws. The accuracy is then guaranteed by the reference pins. The end result leads to the axial tolerance of less than two hundredths of a millimeter.
The modular issue is solved modifying only one of the parts of the structure, the one where the gearbox will be fixed with screws. The exploded view of the complete test bench (fig. 6.9) shows all the parts of the system, and it stresses also the need to have a precise construction.

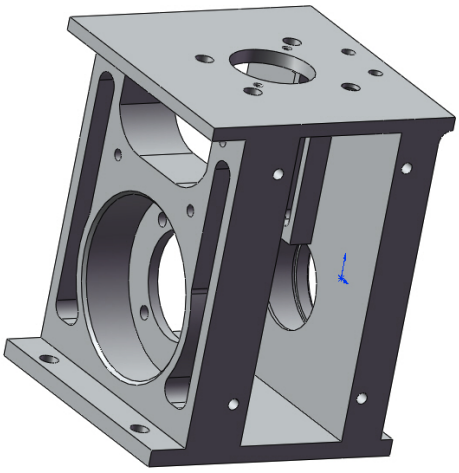

Figure 6.7. Original Aluminum Billet

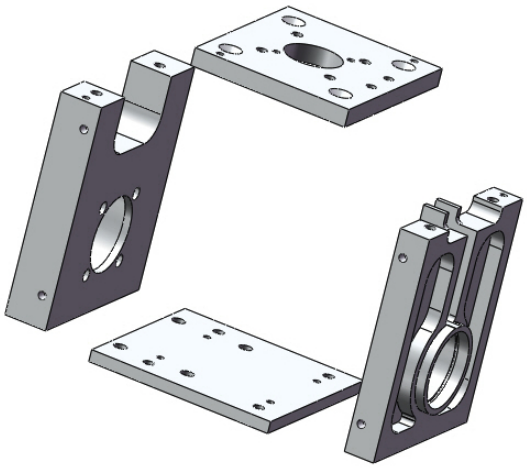

Figure 6.8. Support composed of four parts, easier to assemble

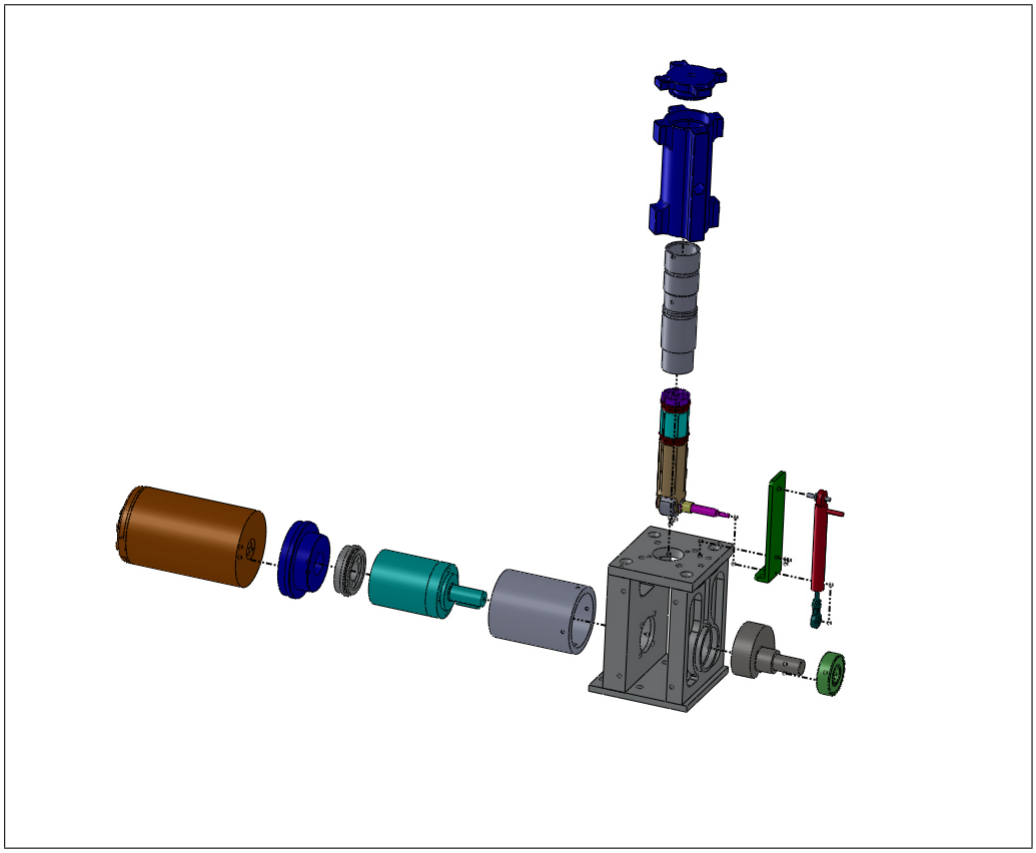

Figure 6.9. Exploded view of the whole system

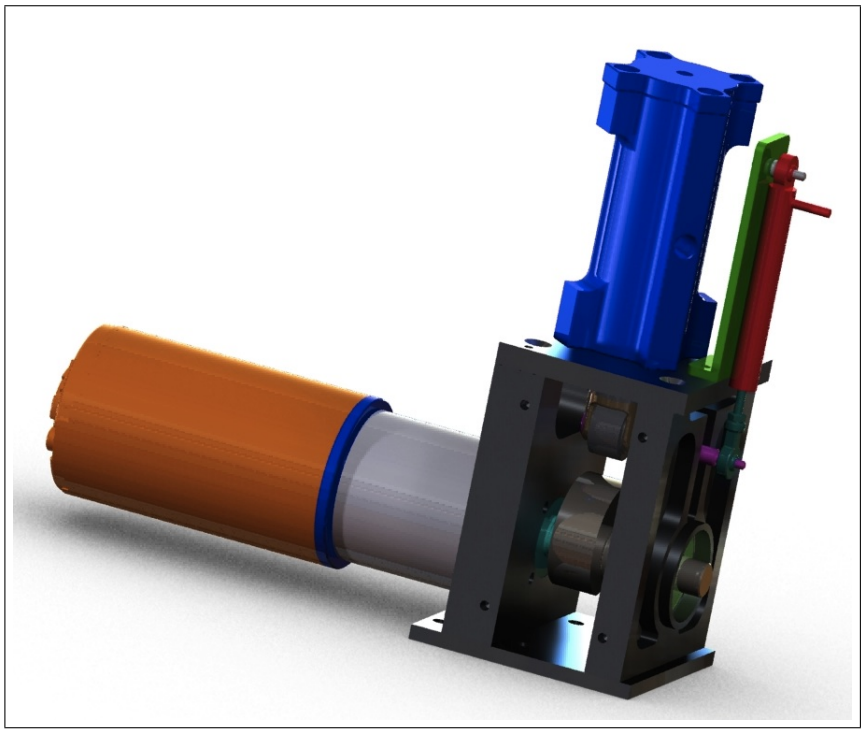

Figure 6.10. Electromechanical System with FISE Motor

6.3 Electromechanical System: Maxon Motor and Gearbox

The second solution was to use a new motor-gearbox with high performances in order to have a reference point for the electromechanical system. The FISE electric motor and the gearbox are substituted with a new motor-gearbox from Maxon. The motor was chosen from the DC Brushed Maxon solutions with less than 250 [W] of nominal power, this was a specification given by SILA Holding Industriale. The system is characterized by having a high torque-to-weight ratio. The parameters of this electric motor (resistance, inductance, inertia, etc.) were used to simulate the clutch actuation with different reduction ratios. Doing so it was possible to adjust the transmission ratio required to ensure high performance. The best opening time was obtained with $\tau = 1/4$. The solution compatible with the motor RE 50 was the gearbox Maxon GP 52. A planetary gear, to ensure high efficiency and high torque capacity.
The specification are listed in table 6.3.

	Electric Motor	**Gearbox**
Name	Maxon RE50 (Brushed Motor)	Planetary Gearhead GP52C
Speed [rpm]	5680	6000[2]
Max Torque[Nm]	8.92	6
η_{MAX} [%]	94	91
Weight [g]	1100	460

Table 6.3. Motor and Gearbox Characteristics

Using the characteristic parameters of these systems, we proceeded to simulate the behavior of the system, to predict the maximum achievable performance. The result is shown in figure 6.11

As said for the previous system, the various components have been modeled using CAD software and the system in figure6.12 was obtained.

[2]Max speed allowed

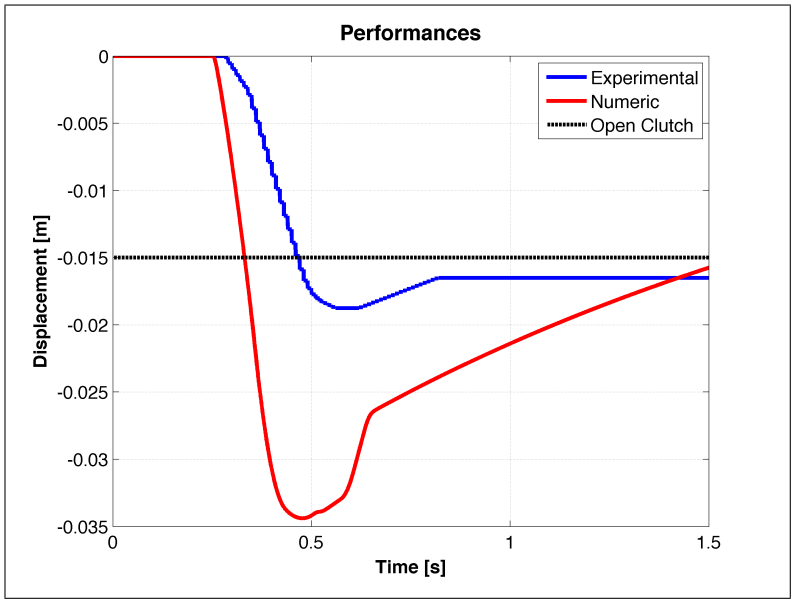

Figure 6.11. Numerical simulation of the system with the Maxon motor-gearbox ($\tau = 1/4.3$); Opening time: 75 [ms]

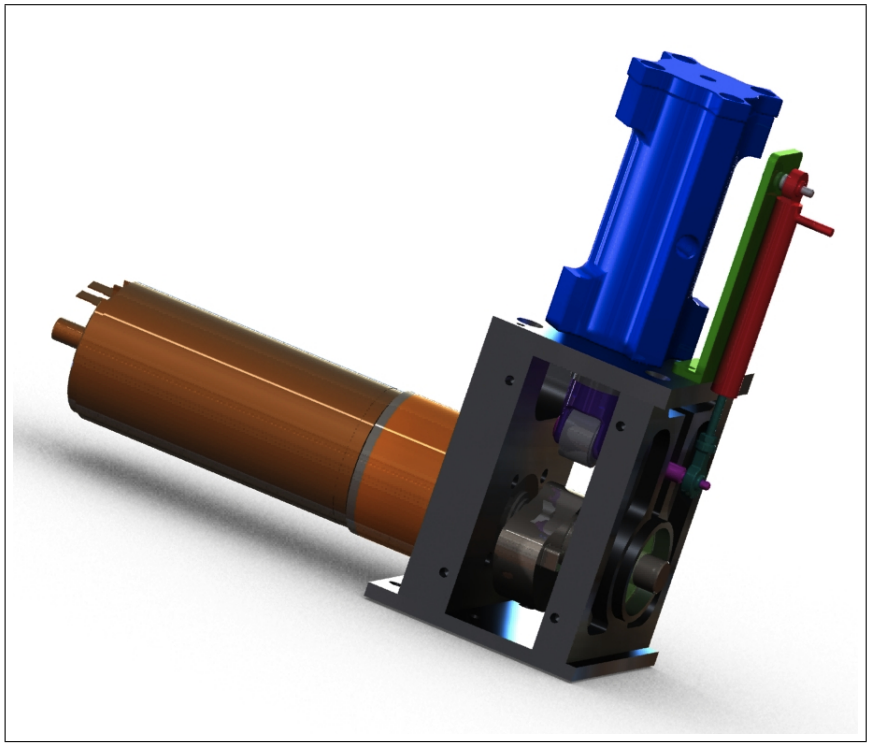

Figure 6.12. Electromechanical System with Maxon Motorgearbox

6.4 Electro-Hydraulic System

The first chapter of the thesis introduces the field of study of electro-hydraulic systems, with particular attention to EHS and EHA systems. These systems are characterized to have more performance than electromechanical systems with the same size and weight. For these reasons, as well as the fact that the center of the LIM-CSPP Polytechnic of Turin has a long tradition of electro-hydraulic applications, we proceeded to design a system for implementing EHS clutch actuation. The key points of the design are:

1. Performance equivalent to or higher than the electromechanical system;
2. More compact and lightweight;
3. Simple construction.

To achieve the aforementioned goals a hydraulic circuit with a limited number of elements is designed, to which were added the components necessary to achieve a high level of security. The components necessary for the engage of the clutch slave cylinder are: Electric motor, pump, circuit and oil tank. The scheme of the final system is shown in figure 6.13

1. **Brushed DC Electric Motor**: this technology was chosen in order to lower the overall cost of the system;
2. **Rigid coupling**: light and compact;
3. **Hydraulic Pump**: the pump displacement is very important, in fact it determines the total ratio between input torque and force over the clutch;
4. **Electro-valve**: the choice was driven by the working power consumption (the lower the better), working pressure and dimensions;
5. **Slave Cilinder**;
6. **Relief Valve**; compact body;
7. **Oil Tank**: At this stage no further study was performed;
8. **Circuit housing**.

In figure 6.13 is shown the hydraulic diagram of the system implementation, as it is known to be associated with the EHS system called Bleed-Off. The operation of the actual system, however, differs from this classification because the system is controlled directly by acting on the electric motor, via an electronic control unit. The operation of the system is the following, when the system receives a signal to disengage the clutch the controller switches the electric motor, which is connected

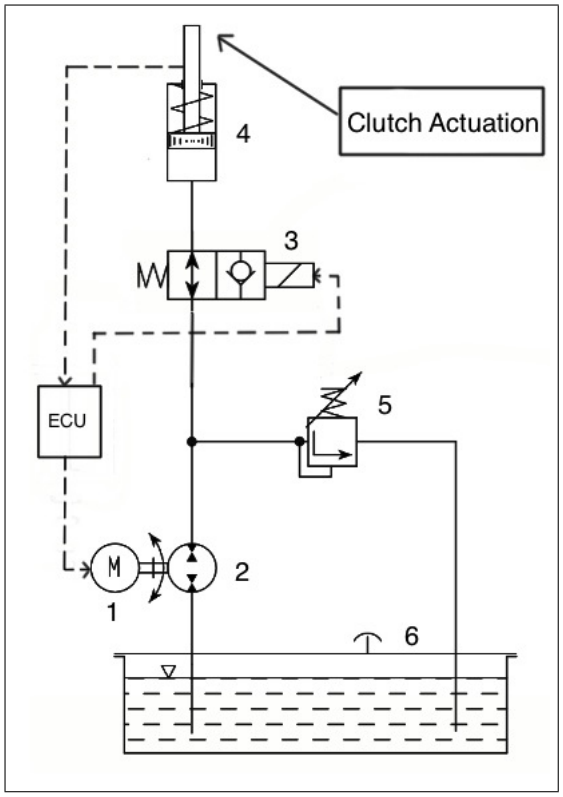

Figure 6.13. Hydraulic Scheme

to the hydraulic pump. The latter provides a flow in order to move the clutch actuator in finite time, less than 100 [ms]. The sizing of the system was done in order to have a disengage time lower than that of the electromechanical solution (section 6.3). The electric motor then provides enough torque to overcome the inertia of the elements along the line of implementation (pump, fluid actuator) and move the clutch spring. The presence of the pressure relief valve is due to the fact that it was necessary to protect the circuit in case of overpressure (even if this condition is difficult to find given the characteristics of the system.)
The servo valve on the other hand has been inserted with a specific purpose, to prevent the continuous operation of the electric motor thus safeguarding the thermal point of view. In fact, the solenoid valve is actuated when it becomes necessary to keep the clutch position, avoiding that the electric motor produces a maintenance torque for a long time. The valve will be used, therefore, as an ON-OFF. Being normally open it will allow fluid to flow in both directions. The moment the clutch is disengaged, if this condition must be maintained for a few tens of seconds (for example at traffic lights) the electro-valve is closed; the fluid trapped between the valve and the slave maintains the pressure level, except for some leakage. The

leakage itself, it is not a problem because in case of pressure drop, the electric motor could be operated to maintain the right pressure level.
This prototype shares with the electro-mechanical system the slave cylinder. Sila used a DOT 4 brake oil as the hydraulic fluid, in order to do minor modification to the test rig the same oil is used.
In fact, hydraulic components use, in general, Buna or Viton soft gaskets (O-rings, etc..). All specification are indicated with hydraulic oil, with a viscosity of 46 [cSt] at 40 [°C], changing the fluid (and hence surface tension) and also the viscosity, it change the leakage and operational behavior. The system will use what is commonly called "brake fluid", which actually has little to do with the normal oil and definitely have to take into account the different viscosity of hydraulic oil reference. The material for the soft seal for these fluids is the EPDM, it could be said that from the point of view of the demonstrator Viton can be used, but if wearing has to be taken into account probably a further study must be done.
In table 6.4 are shown electric motor and pump specifications. This two component were defined using the numerical model in order to provide the right torque (motor) and the right rate flow (pump). Otherwise, the rigid coupling and the valves were defined by their overall dimensions.

	Motor		**Hydraulic Pump**
Name	Maxon RE40 24 [V] (Brushed Motor)	**Name**	Marzocchi UK 0.5 D 1.60
Speed [rpm]	7580	**Max Speed [rpm]**	5000
Max Torque [Nm]	2.28	**Max Pressure [bar]**	190
η_{MAX} [%]	91	**Displacement [cm^3/rev]**	1.25
Weight [g]	480	**Weight [g]**	900

Table 6.4. Motor and Pump Characteristics

The parameters of the electric motor and the pump are introduced in the numerical model in order to find out the opening time. The model takes into account both the electrical characteristics (resistance, inductance) and mechanical (inertia) of the electric motor, while as regards the pump, the parameters considered are the displacement, the damping and inertia. Some parameters were found in the data sheet, others were guessed in order to run the simulation.
In figure 6.14 is shown the behavior of the numerical model (red) with respect to the actual SILA prototype. In fact a this point of the analysis all the viscous friction parameters are unknown, they must be guessed.

To build the prototype the components cited above are needed, this part of the project was about finding the best solution in terms of performances, dimensions, weights and costs.
First step was to find a coupling in order to connect the electric motor and the pump. From the design point of view it is important to choose a low inertia

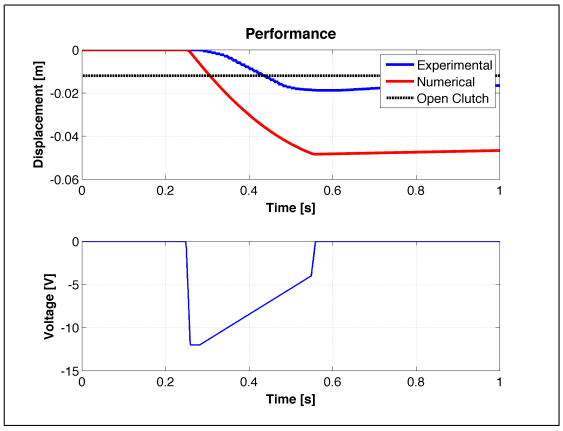

Figure 6.14. Top: Hydraulic system performances, dotted black line is the open clutch displacement, the modeled hydraulic system opens in 70 [ms]: Bottom: Input voltage

coupling with a axial degree of freedom, in order to avoid problems due to non-coaxiality between the motor and pump shafts. The component selected is the Panamech MULTI-BEAM BC24.
Looking at the scheme in figure 6.13 two valves have to be selected: an electro-valve and a relief valve for safety.
Consider the waiting at the traffic light, a very onerous condition, in which the system must maintain the clutch engaged for a period of time which can be of several minutes. In the event that it were the electric motor to provide power to maintain the clutch spring compressed, it is clear that there would be a high energy consumption. In this condition becomes essential to have a valve, which when operated allows the pressure management. For this task has been selected the valve, shown in figure 6.15, with its coil, figure 6.16. This two components were small enough to maintain compact the overall dimensions of the system. The total weight of the valve and the coil is 290 [g], and the power needed by the system is 20 [W].

In order to design a safe hydraulic system the circuit needs a relief valve. In this case the pressure maximum value is defined by the mechanical constraints of the clutch actuation. The force acting on the slave is due to the compression of the spring, its maximum value, in the case of a small car clutch, is about 800 [N] that gives 80 [bar]. Nonetheless a compact relief valve is considered, see image 6.17.

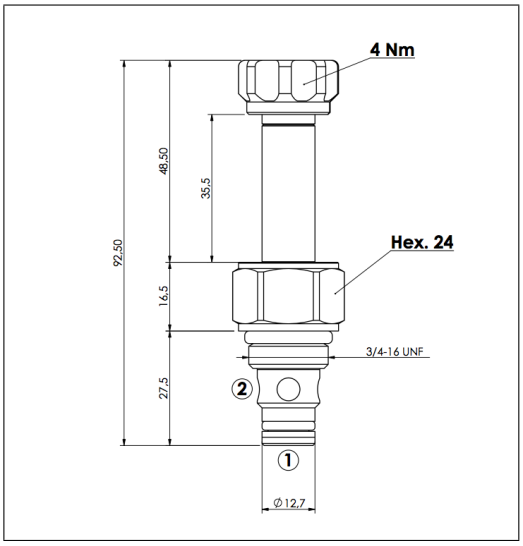

Figure 6.15. Atlantic Fluid Tech: CEBP 040 NAFN, Max pressure: 350 [bar]

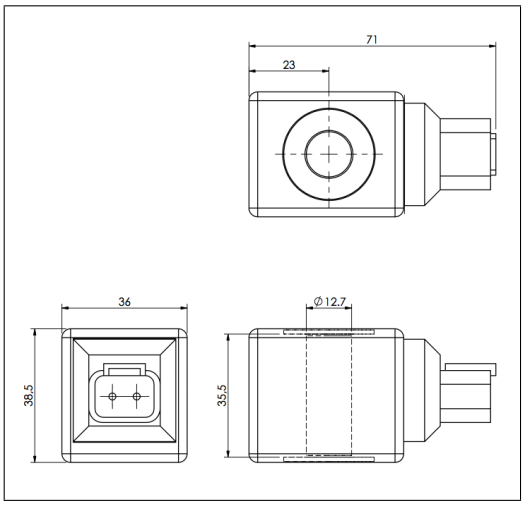

Figure 6.16. Atlantic Fluid Tech: COIL M7, Voltage: 12 [V], Current: 1.62 [A]

6.5 Mechanical Assembly

All the aforementioned components must be housed and connected following the key features pictured in section 6.1. The present section describes the solution adopted. In order to have a light and compact component the first consideration to be done is to have an aluminum billet where drill the circuit. In fact this solution, in figure 6.18, is useful, furthermore, to reduce the gap between the motor and pump shafts. The overall dimension are defined by the components

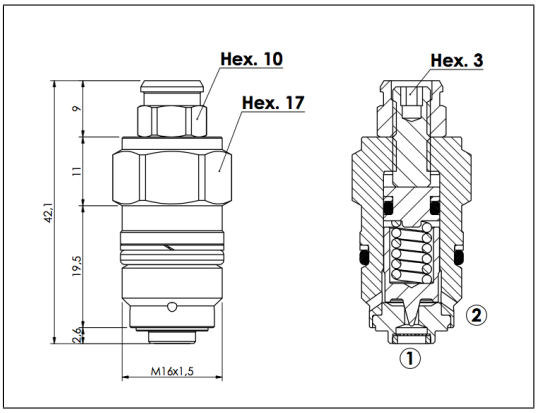

Figure 6.17. Atlantic Fluid Tech: Relief Valve, Weigth: 50 [g]

and the thickness of the walls to withstand the hydraulic pressure during the opening procedure.
The material chosen for its mechanical properties and the containment of the weight is ERGAL 7075 T6.

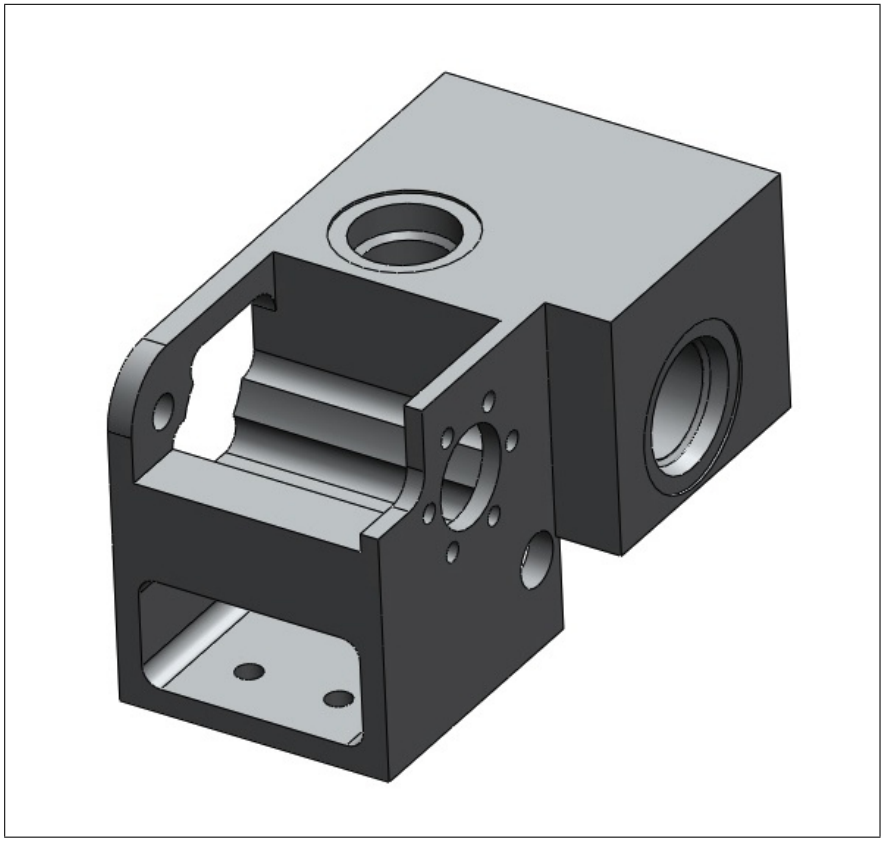

Figure 6.18. Housing

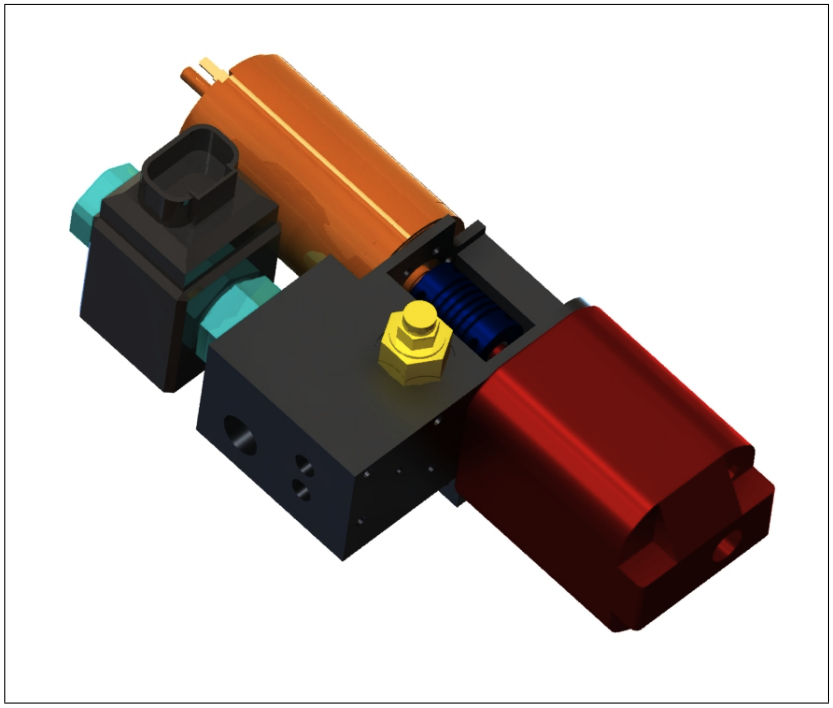

Figure 6.19. Assembly Rendering

6.6 CFD Analysis

The hydraulic component (fig. 6.18) that houses the main circuit is very important to keep the system compact, however it is very important to check this design in order to avoid problems during test. To do so, a CFD analysis is done; the tool chosen is Comsol Multiphysics.
This tool is a powerful software that is able to compute multi physics problems such as Thermal Fluidodynamics, Electrochemistry and Electromagnetics simulations. For this analysis the Comsol CFD tool is chosen.
The model is built using the exact geometry imported from Solidworks using a STEP file.

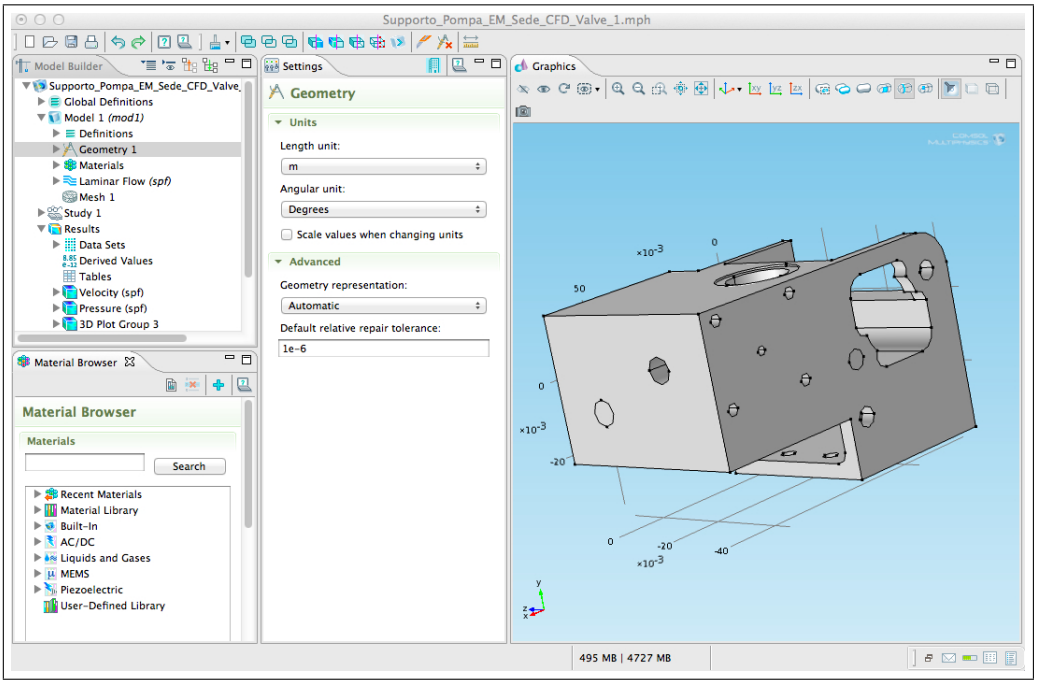

Figure 6.20. Imported model on Comsol

Using the model shown in figure 6.20, the first step was to choose the study to perform: Single-Phase Laminar Flow, Stationary. The characteristics of the DOT 4 brake oil, used by SILA, were approximated using a standard material in the Comsol library: Transformer Oil
The fluid domain is created using the command Cap Faces, that is able to identify the circuit. The mesh of the system is made using default configuration for Comsol, taking into account the analysis that must be performed.

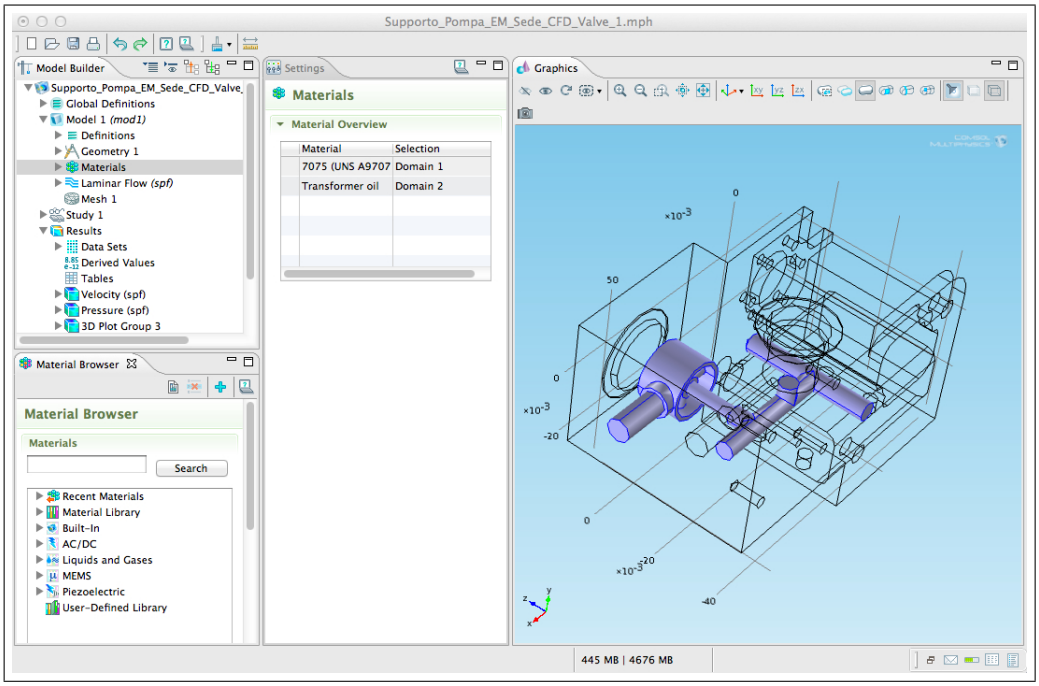

Figure 6.21. Model materials: Aluminum and Oil

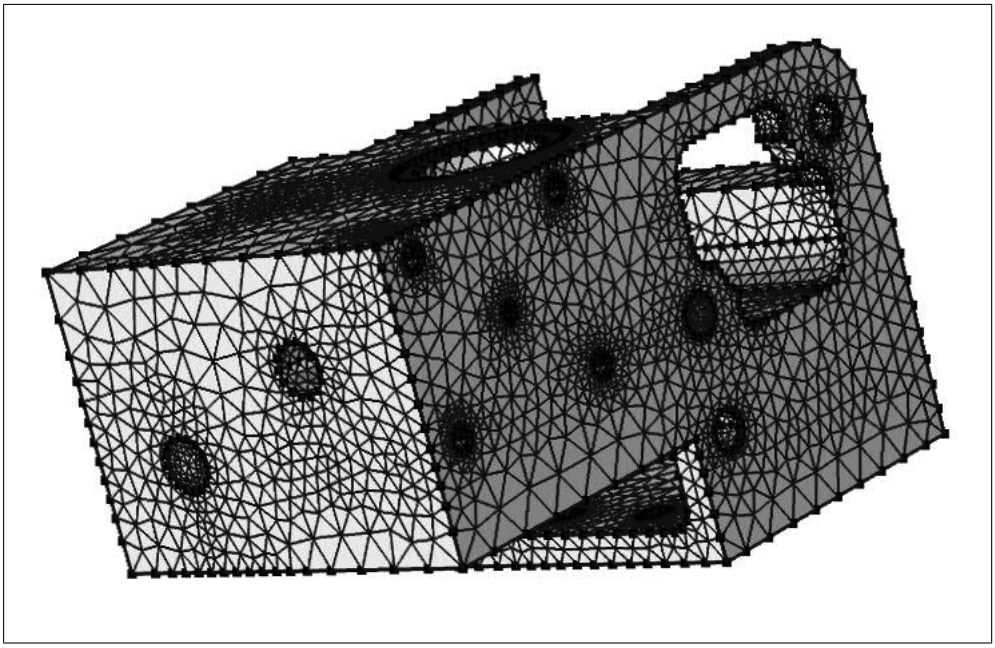

Figure 6.22. Meshed model

The results are shown in figure 6.23 where it is possible to see that the pressure drop from the Inlet to the outlet of the circuit it is small. It must be underlined that the circuit diameter is kept constant where possible.

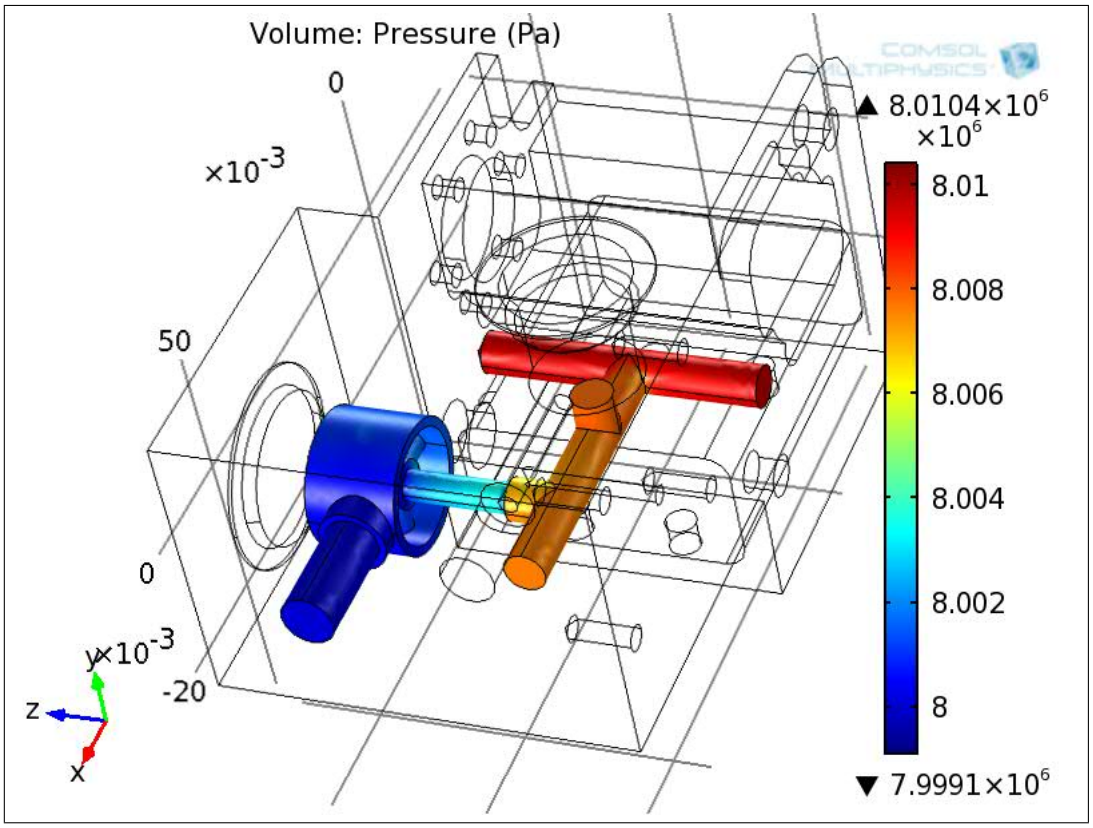

Figure 6.23. Oil Pressure in the circuit

Part III

Experimental test

Chapter 7

Experimental test and Results

The final part of this thesis focuses on the analysis of results obtained through a series of experimental tests carried out on prototypes built according to plans explained in previous chapters.
The test bench is characterized with minimal changes to accommodate the three prototypes. They, as mentioned above, are designed to be interchangeable, having the common flow toward the slave cylinder which controls the clutch actuation. The test bench is equipped with the hydraulic connection between the master (in the case of electromechanical systems) and the slave, which moves the actuator. The latter works on a linear spring (see image 7.2) that simulates the load given by the spring of the clutch that works on the slave cylinder. From previous tests carried out at the company Sila, the load applied in limited wear condition is about 800 [N]. The test bench is as in figure 7.1.

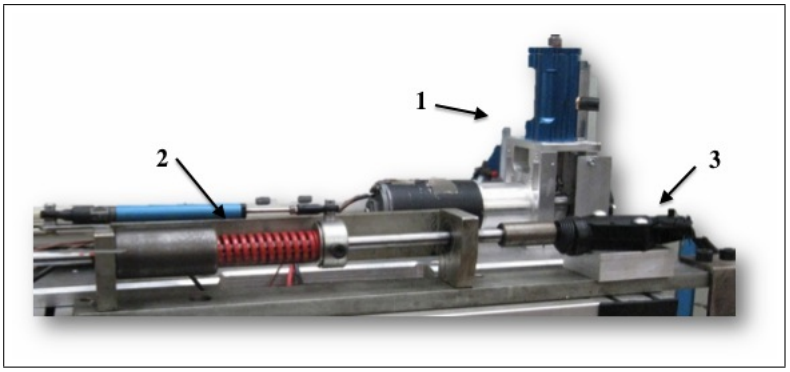

Figure 7.1. Test bench with the FISE electric motor

The main components are:

1. Fise Motor with gearbox, cam and master cilinder;
2. Slave;
3. Linear spring (58 [N/mm]) and potentiometer.

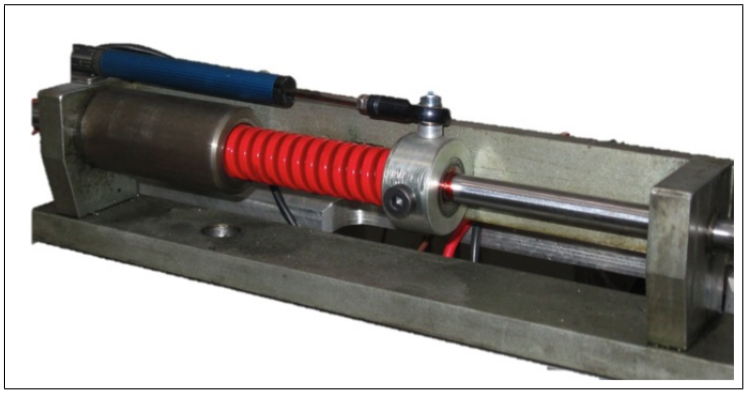

Figure 7.2. Linear Spring connected to the slave

The design of this bench test led to have interchangeable systems with an easy mounting and un-mounting. As you can see in figure 7.3 it is possible to substitute only the bottom part of the system avoiding to purge twice the hydraulic part.

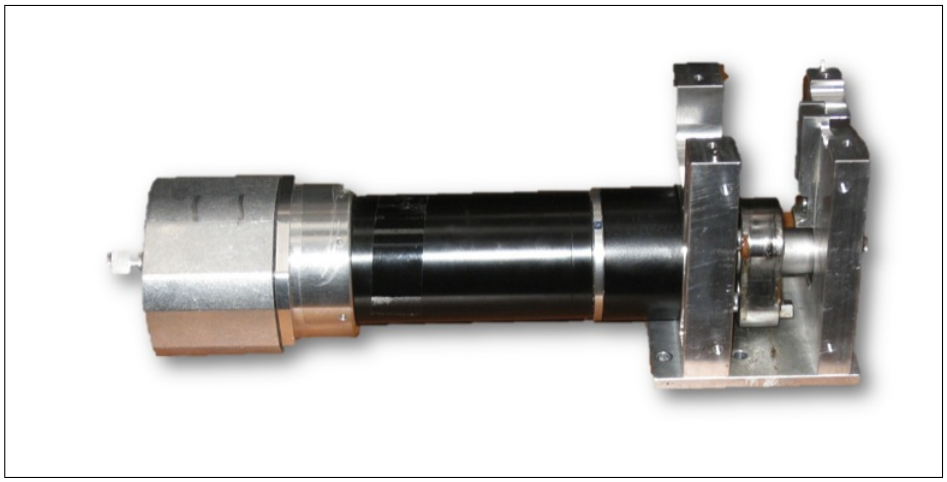

Figure 7.3. Maxon System bottom part

7.1 Electromechanical Systems

The goal of the project was to achieve clutch opening times lower that 200 [ms], so in order to check the performances, the EMA systems were fed with duty cycle of voltage in open loop. The results shown in the following pictures are about the maximum performance of each one.

7.1.1 Electromechanical System: FISE

Starting with the FISE electromechanical system, it was important to understand, also the system power consumption. In fact as the voltage is known it is important to take into account the current value. In figure 7.4 is shown the experimental result, it is important to notice that improved system is, indeed, faster that the previous version. This is due to the fact that the torque provided from the FISE motor was more than enough and the reduction ratio was too high. This could be important to have a non reversible system, but in this case the damping factor was too big and the overall performances were low. In figure 7.4 is shown also the current produced by the electric motor in order to keep the clutch position. The FISE solution needs 35 [A] and it is obvious that this value is too high and that involves a waste of energy is not negligible. A possible solution is the use of a magnetic brake.

- Same Electric Motor;
- Gearbox with lower ratio and lower inertia;
- Low inertia cam.

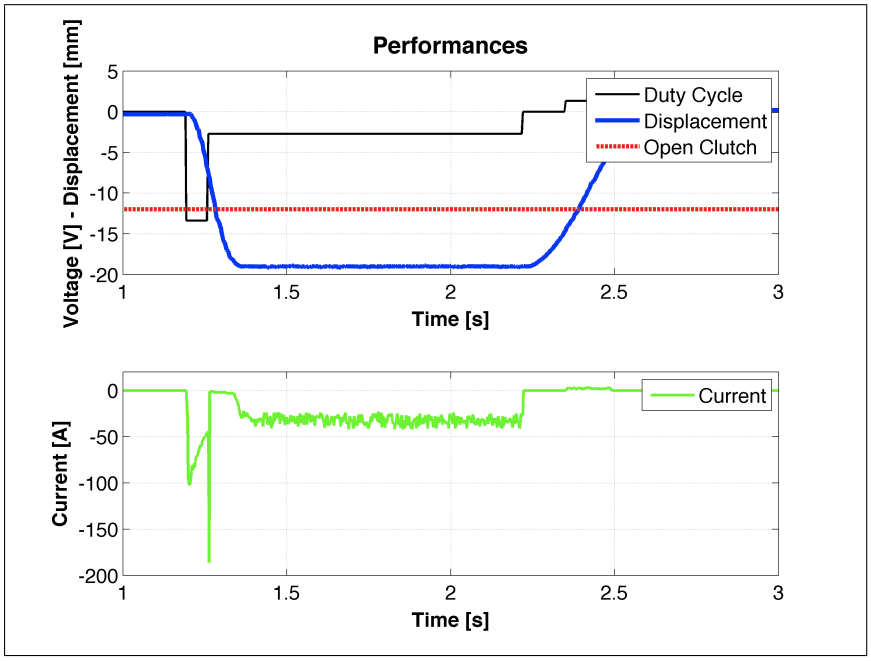

Figure 7.4. Top: Open Clutch is set at 12 [mm], the system opens in 148 [ms] following the voltage DC; Bottom: the current has a peak near 200 [A], but the holding current is about 35 [A]. Maximum voltage: 13.5 [V]

7.1.2 Electromechanical System: Maxon

The FISE motor could provide a solid performance, but in order to open the clutch in less than 100 [ms] it is necessary to use an electric motor with low inertia and high efficiency. During the design stage a lot of motor were analyzed but the best solution was the Maxon RE 50, an DC motor with high torque and efficiency. In order to meet the speed and torque specification of the clutch actuation the electric motor was combined with a gearbox (GB 52) with reduction ratio: 4.3.
The opening times achieved by this system are shown in figures 7.5 and 7.6:

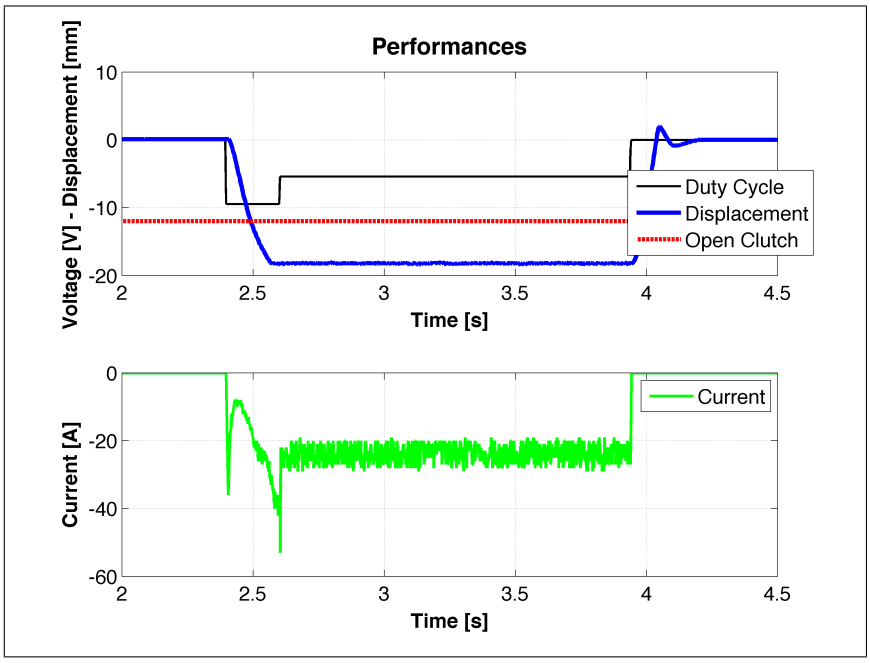

Figure 7.5. Top: Open Clutch is set at 12 [mm], the system opens in 105 [ms] following the voltage DC; Bottom: the current has a peak near 60 [A], but the holding current is about 23 [A]. Maximum voltage: 13.5 [V]

Images 7.5 and 7.6 show that the Maxon system has high performance. The opening procedure takes less than 100 [ms]. Another important consideration can be drawn from the analysis of the holding current patterns. The value of the latter is around 20-25 [A], allowing energy consumption lower than the FISE configuration.
The RE 50 motor could work with 24 [V], but the tests are performed using the voltage delivered by the car battery (more likely situation).

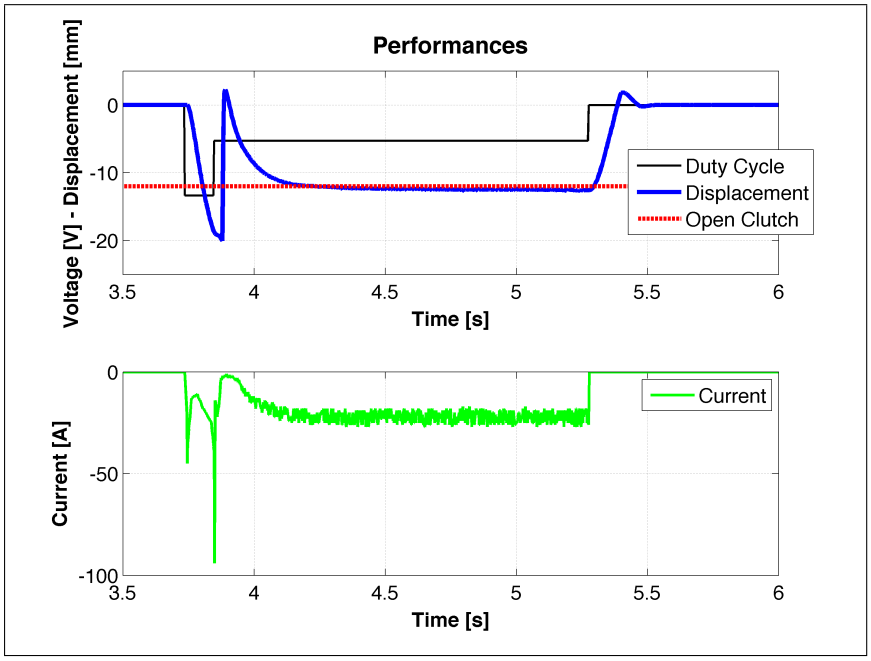

Figure 7.6. Top: Open Clutch is set at 12 [mm], the system opens in 70 [ms] following the voltage DC; Bottom: the current has a peak near 100 [A], but the holding current is about 23 [A]. Maximum voltage: 9.5 [V]

7.2 Electro-Hydraulic System

The last experiment is done with the Electro-Hydraulic system, in figure 7.7 all the hydraulic components are shown. The real system mounted, however, is shown in fig. 7.8; it could be confronted in term of volume occupation, with the high performance EMA system (see fig. 7.9).

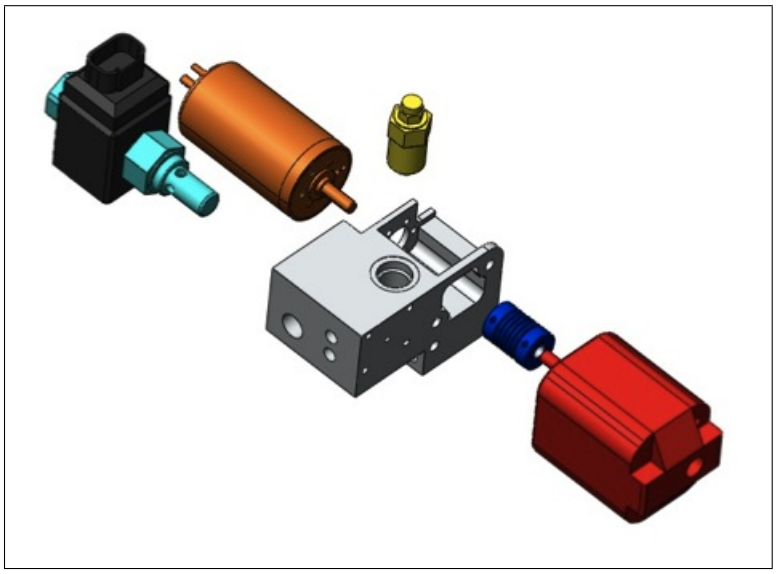

Figure 7.7. Exploded view of the hydraulic system

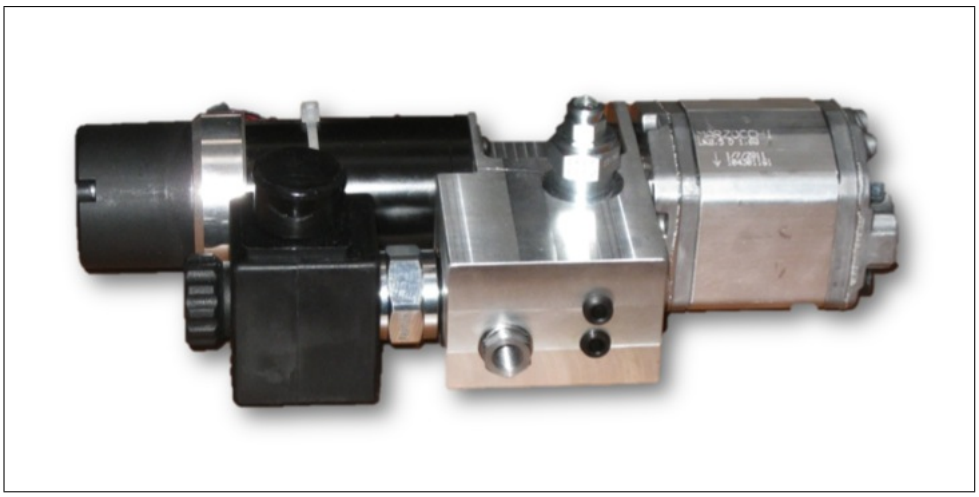

Figure 7.8. Hydraulic system mounted

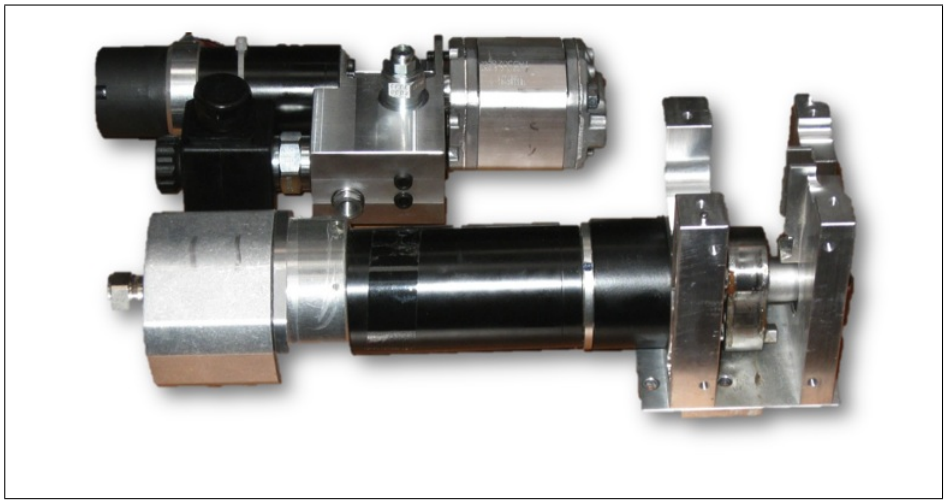

Figure 7.9. Comparison between the hydraulic and mechanical solution

In figure 7.10 the results of the hydraulic system are shown.
The hydraulic system opens the clutch in 130 [ms], but it is useful to take into account the system initial delay. In fact the system doesn't move for 30 [ms] after the voltage input, this is probably because of the stiction of the pump and its low efficiency at low speeds. In the model used to design the system it wasn't taken into account.
The current used to maintain the open clutch condition is approximately 20 [A]. But in the case in which the solenoid valve is operated, the condition is met by reducing the use of energy. In fact, the solenoid valve has a rated power of only 20 [W].

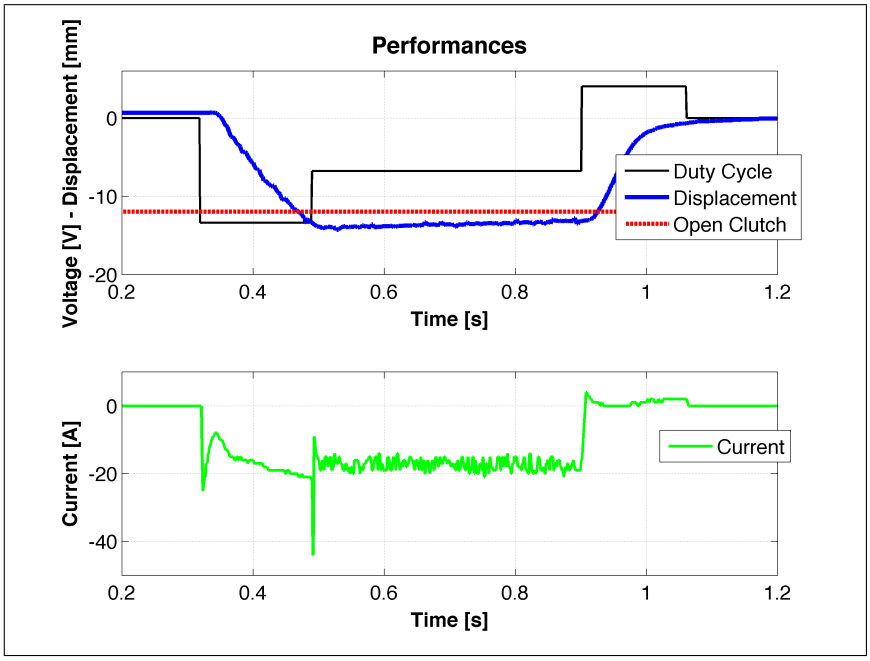

Figure 7.10. Top: Open Clutch is set at 12 [mm], the system opens in 130 [ms] following the voltage DC; Bottom: the current has a peak a little over 40 [A], but the holding current is about 18 [A]. Maximum voltage: 13.5 [V]

Chapter 8

Parameter Identification

8.1 Non Linear Electromechanical Model

A non linear model was built in Matlab&Simulink in order to take into account the behavior of the eccentric.
The modified cam used in the electromechanical prototypes kept the original profile as it is shown in figure 6.3: the goal of this model is to match the real displacement of the master cylinder and also to reproduce the actual torque seen by the cam. The torque varies with the angle of incidence of the force acting on the cam (see figures 8.2 and 8.3).

The non linear model is needed in order to identify the model parameters, unfortunately, the State Space representation doesn't allow to have a non linear model. The idea was to separate the whole system in tree sub-systems, fig. 8.4:

1. Mechanical part with inertial properties and friction coefficients of the electric motor and gearbox;
2. Non linear cam;
3. Hydraulic model of the Master and Slave system and clutch.

8.2 Electric Motor and Gearbox

The State Space system of this part is written down using Bond Graph technique and it has only one state related to the inertia of the electric motor.

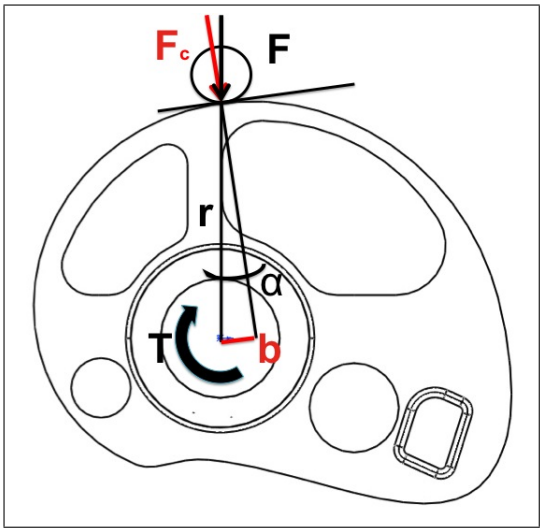

Figure 8.1. Force acting on the cam

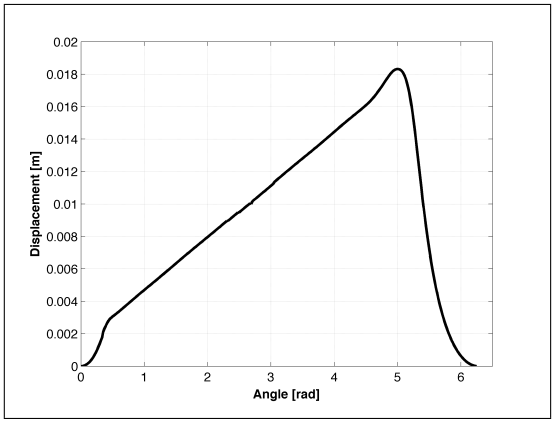

Figure 8.2. Actual displacement

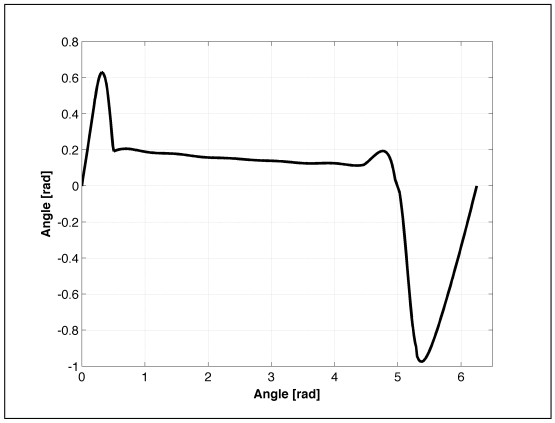

Figure 8.3. α

The state equation (8.1) takes into account the inertial properties:

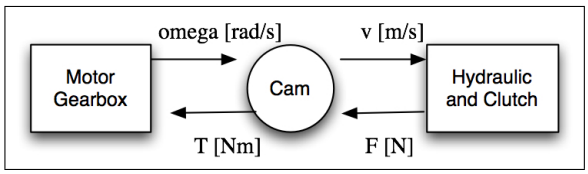

Figure 8.4. Non linear model

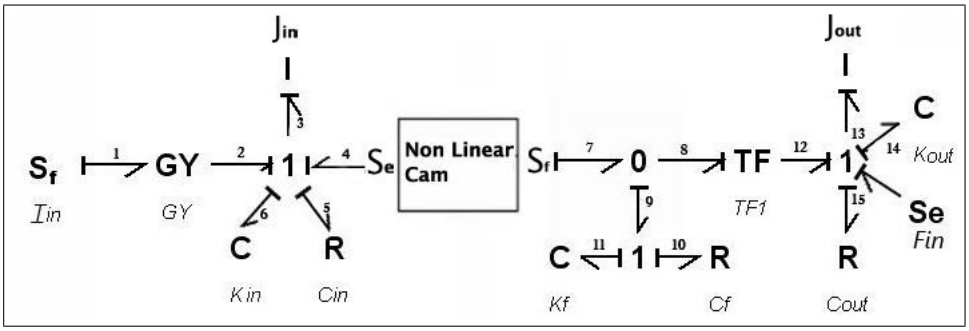

Figure 8.5. Bond-Graph with non line cam

$$\dot{p}_3 = -\frac{C_{in}}{J_{tot}} p_3 + Ki + \tau\, T_{CAM} \left(\frac{J_{in}}{J_{tot}} \right) \tag{8.1}$$

In the equation (8.1) is possible to identify the input from the electric motor, **i** and the torque from the eccentric T_{CAM}. From the Bond-graph of the system the total inertia of the motor-gearbox part is:

$$J_{tot} = J_m + J_{gb} + \tau^2 J_{CAM} \tag{8.2}$$

The State Space model with its A, B, C and D matrix is the following:

$$\{\dot{p}_3\} = \left[-\frac{C_{in}}{J_{tot}} \right] \{p_3\} + \begin{bmatrix} \frac{K J_{in}}{J_{tot}} \\ \frac{\tau J_{in}}{J_{tot}} \end{bmatrix} \begin{Bmatrix} i \\ T_{CAM} \end{Bmatrix} \tag{8.3}$$

$$\begin{Bmatrix} T_m \\ \omega_{CAM} \end{Bmatrix} = \begin{bmatrix} 0 \\ \frac{\tau}{J_{in}} \end{bmatrix} \{\dot{p}_3\} + \begin{bmatrix} K \\ 0 \end{bmatrix} \begin{Bmatrix} i \\ T_{CAM} \end{Bmatrix} \tag{8.4}$$

8.3 Non Linear Cam

The non linear cam implemented in the model takes into account the real radius of the cam. The fundamental hypothesis is to have the continuos contact between cam and cylinder. Moreover, the component force ($\mathbf{F}_c$) acting on the cam produces a moment the is variable with the angle α; the lever **b** is related to the value of the actual radius **r**. As can be seen in figure 8.1:

$$F_c = F \cos\alpha \quad \rightarrow \quad b = r \sin\alpha \tag{8.5}$$

$$T = F_c b \tag{8.6}$$

The angle α and the actual displacement are shown in figure 8.3, these values are highly non linear and the result is that the simulation is quite longer.

8.4 Hydraulic fluid and Clutch

The hydraulic system and the clutch are modeled as shown in chapter 3, the unique difference is due to the fact that the non linear spring of the real system is substituted by a linear one in the test rig. The model is modified in a simple way: the input force due to the non linearity is neglected, the stiffness of the linear spring is 5.88 [kg/mm]. The Bond-Graph equations can be found in appendix A.4. The result in term of Simulink model is shown in figure 8.6 and 8.7.

$$\begin{Bmatrix} \dot{q}_4 \\ \dot{p}_8 \end{Bmatrix} = \begin{bmatrix} 0 & \frac{p_8}{\tau_2\, m_{out}} \\ \frac{K_f}{\tau_2} & -\left(C_{pist} + \frac{C_f}{\tau_2}\right)\frac{1}{m_{out}} \end{bmatrix} \begin{Bmatrix} q_4 \\ p_8 \end{Bmatrix} + \begin{bmatrix} \tau_1 & 0 \\ \frac{\tau_1 C_f}{\tau_2} & -1 \end{bmatrix} \begin{Bmatrix} v_{lin} \\ F_{clutch} \end{Bmatrix} \tag{8.7}$$

$$\begin{Bmatrix} v_{slave} \\ F_{CAM} \end{Bmatrix} = \begin{bmatrix} 0 & \frac{1}{m_{out}} \\ \tau_1 K_f & -\frac{\tau}{\tau_2}\frac{C_f}{m_{out}} \end{bmatrix} \begin{Bmatrix} q_4 \\ p_8 \end{Bmatrix} + \begin{bmatrix} 0 & 0 \\ \tau_1^2 C_f & 0 \end{bmatrix} \{v\} \tag{8.8}$$

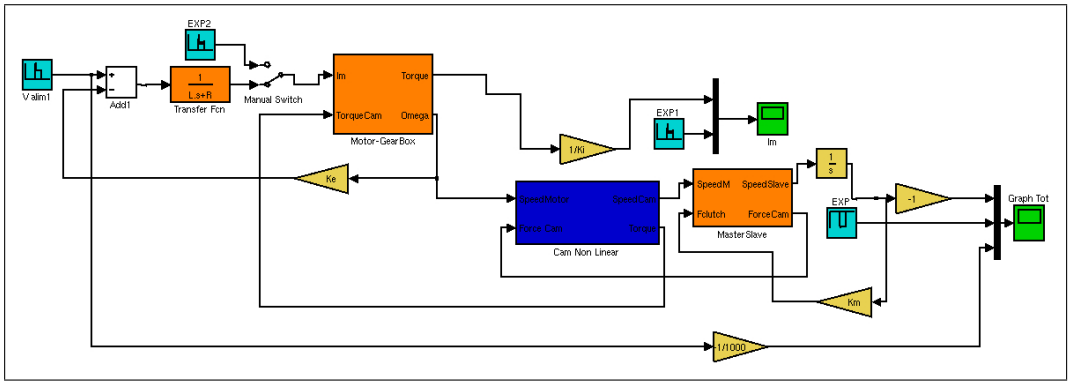

Figure 8.6. Simulink model: whole system

This model is quite similar to the original one, but at this point, it was impossible to neglect the eccentric non-linearity. It could be used either for the system with

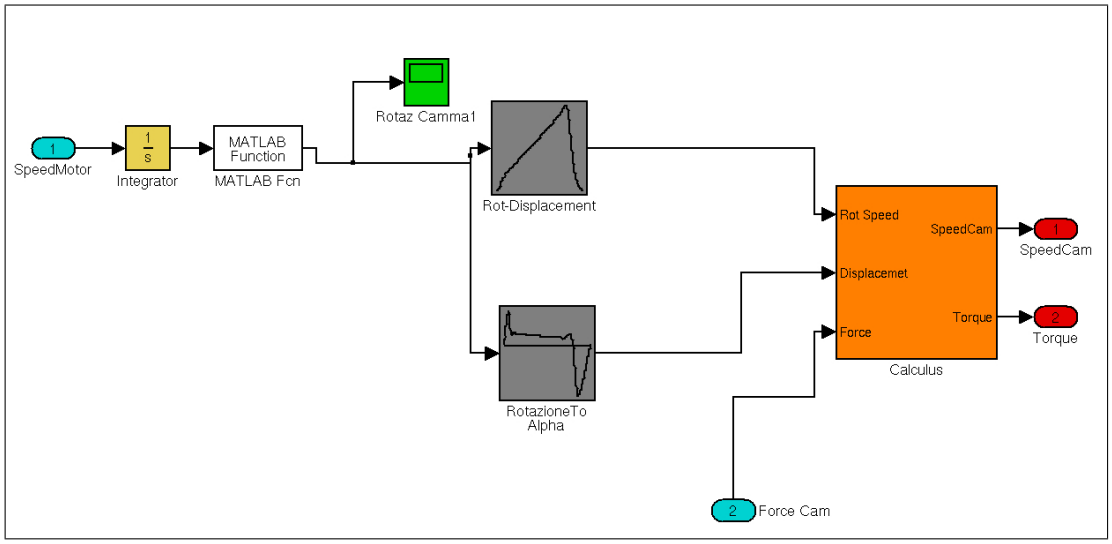

Figure 8.7. Simulink model: eccentric

the FISE motor and the Maxon gearbox and for the Maxon Motor-Gearbox solution. The different parameters are defined in the file .m that is used to setup the simulation.

8.5 Parameter Identification: EMA Systems

The model explained in the previous section is needed to perform the parameter identification of the system. To do so the voltage Duty Cycle is used as model input; the parameters that are chosen to be changed are those that could be considered unknown:

- Motor Resistance (the values measured by multimeter differ from the data-sheet);
- Motor and Gearbox Viscous Friction;
- Fluid Viscous Friction;
- Master and Slave Cylinder Viscous Friction.

In figure 8.8 is shown the best numerical approximation done for the FISE system, using the parameters values in table 8.1.

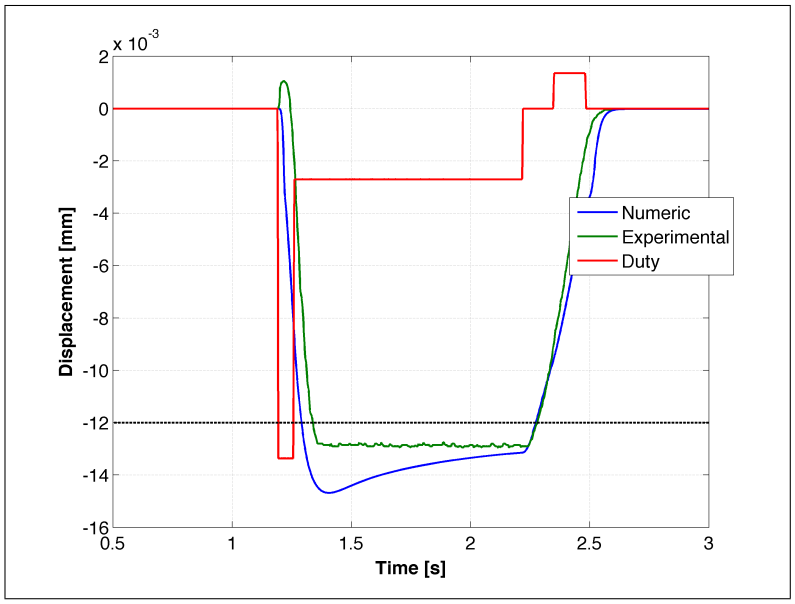

Figure 8.8. Numeric approximation

This model works fine with the data sheet resistance of the motor (in fact the value measured using a multimeter is close, R = 0.2 [Ω]). The values of the frictions were found starting from the light damped system. The slave viscous friction was identified using the hydraulic system model, see section 8.6.
With the same technique it is performed also the simulation of the high performance electro mechanical system. The results are shown in figure 8.9.

Parameter [unit]	Value
Motor resistance [ohm]	0.133
Motor-Gear Friction [Nms/rad]	$16e^{-4}$
Fluid Friction [Ns/m^5]	6.8e^{11}
Piston Friction [N/s]	2e^{-3}

Table 8.1. Parameter identified for the FISE solution

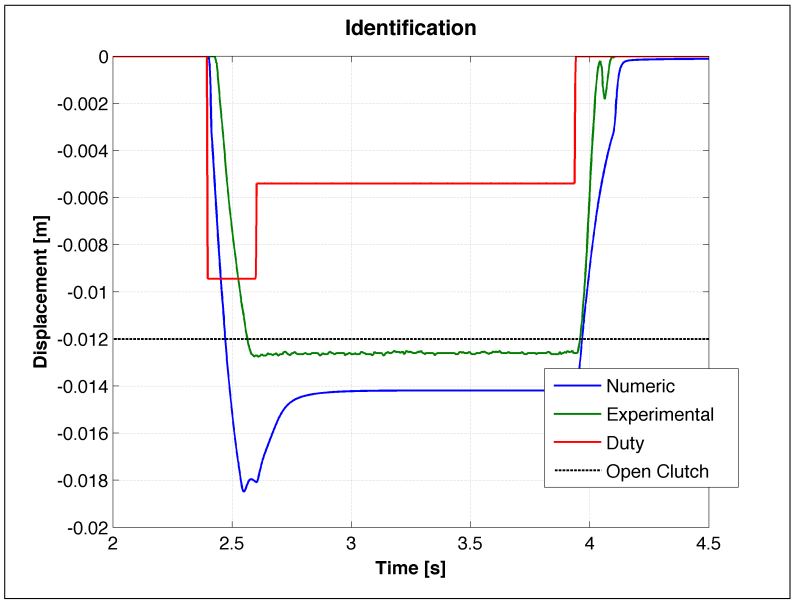

Figure 8.9. Numeric approximation

Parameter [unit]	Value
Motor resistance [Ω]	0.309
Motor-Gear Friction [Nms/rad]	$4e^{-3}$
Fluid Friction [Ns/m^5]	6.8e^{11}
Piston Friction [Ns/m]	2e^{-3}

Table 8.2. Parameter identified for the high performance solution

8.6 Parameter Identification: Electro-Hydraulic System

The identification performed over the Electro-Hydraulic system was done using the model described in chapter 5. In this case there wasn't the non linear eccentric to take into account.
The identification was done starting from the non damped system and then some damping parameters were guessed and others were identified using experimental data. The damping parameters in the model are:

- Motor-Pump friction;
- Fluid damping parameter;
- Slave actuator friction;

In figure 8.10 is shown the numerical response (green line)

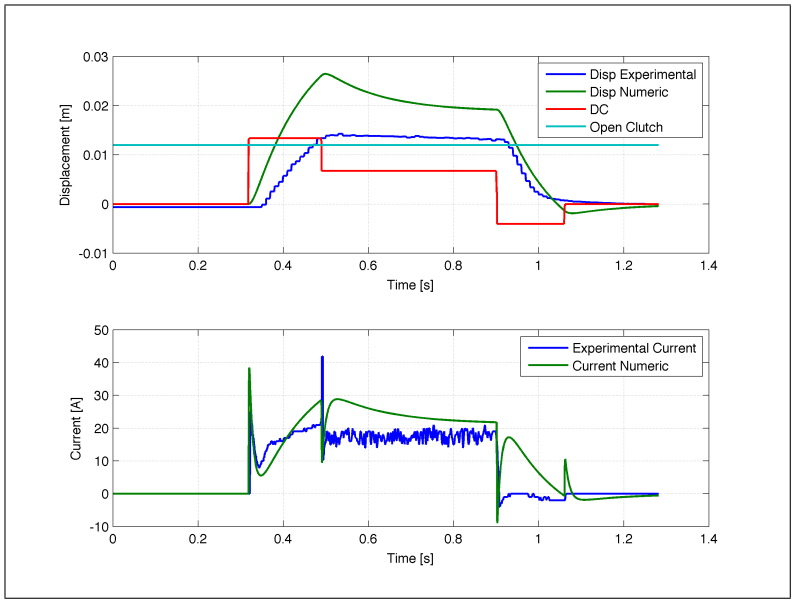

Figure 8.10. Top: From the Duty Cycle in input (red line) the numeric response of the model in green. Bottom: Numeric Current in green and experimental in blue.

The second step was to find the value of the Motor-Pump friction, this was possible dating a simple test: connect the outlet port directly to the tank and supply constant voltage. In this case the rotational speed of the system could be considered constant and the only force acting against the motor torque is given by

the motor-pump friction. The experimental data produced by this test were then matched with the numerical ones. In the numerical model in order to simulate the connection to the tank the slave actuator part were neglected.
In figure 8.11 the numerical current equals the experimental RMS value, the friction factor is $C_{MP} = 8e^{-4}$ [Nms/rad]. The identified value is valid under the assumption of considering only the stationary condition neglecting the transients.

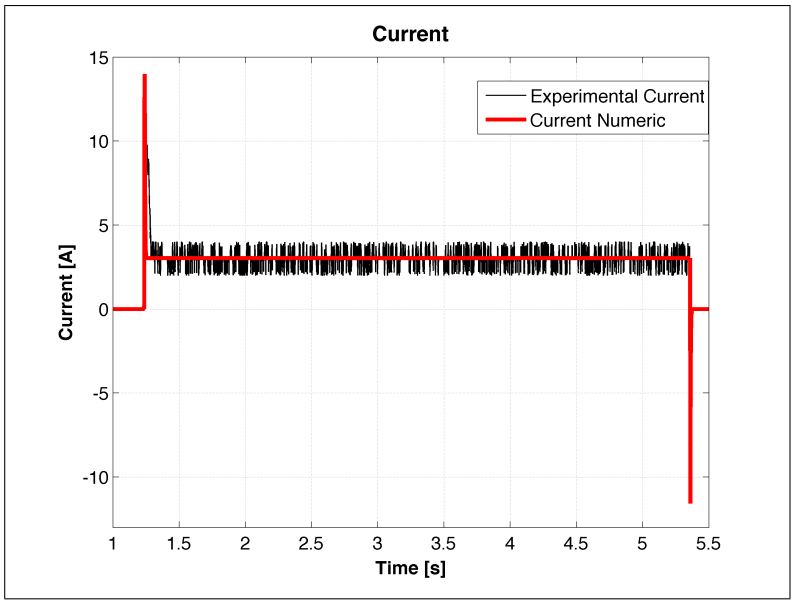

Figure 8.11. Numerical Current (black line) equals the experimental current

As regards the value of the viscosity of the fluid, its value is taken from Pristerá and Romeo works [11, 12]. All the parameter values are shown in table 8.3. The identification result is presented in figure 8.12

Parameter [unit]	Value
Motor resistance [Ω]	0.4
Motor-Pump Friction [Nms/rad]	$4e^{-3}$
Piston Friction [Ns/m]	$2e^{-3}$
Fluid Friction [Ns/m^5]	$6.8e^{11}$

Table 8.3. Parameter identified for the hydraulic solution

Tn order to understand the weight of the viscous damping on system performance is possible to make an energy analysis. Having defined the total value of the

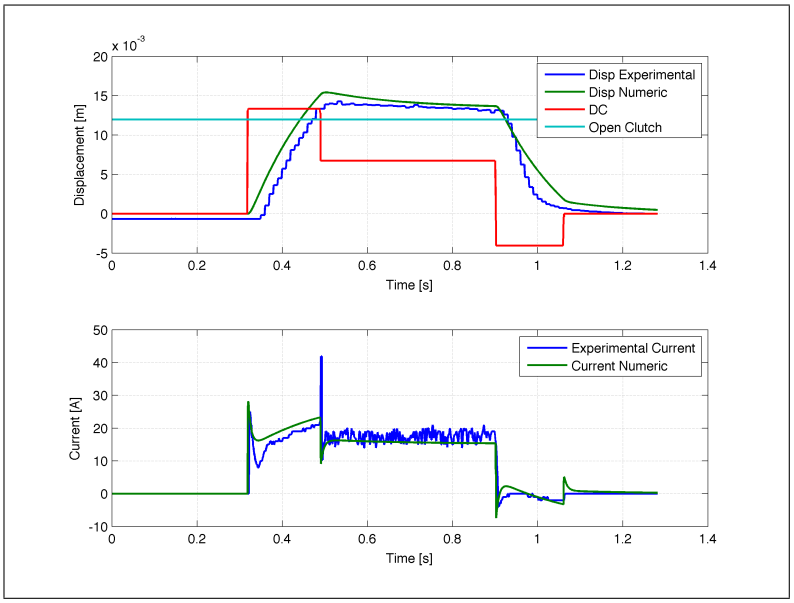

Figure 8.12. Top: From the Duty Cycle in input (red line) the numeric response of the model in green. Bottom: Numeric Current in green and experimental in blue.

transmission ratio between the pump and the cylinder prejudice as τ_{total}, assuming non losses in the circuit:

$$Q_{in} = Q_{out} \quad \rightarrow \quad D_{pump}\omega = A_{slave}v \tag{8.9}$$

$$\tau_{total} = \frac{D_{pump}}{A_{slave}} = \frac{V}{\omega} \tag{8.10}$$

Q_{in} and Q_{out} are the volumetric flows in input (from the pump that rotates with speed: ω) and output (the hydraulic fluid that moves at v). So the transmission ratio is defined by the pump displacement D_{pump} and the piston area (A_{slave}). Under the hypothesis that the energy dissipated by the system is entirely due to the friction of the motor-pump system, the relation in eq. (8.11) is valid. The total energy could be written related to the speed of the slave actuator (8.12). From these relations it results that the value of the pump damping is predominant in relation to the other parameters being a function of reduction ratio squared.

$$E_{loss} = \frac{1}{2}C_{pump}\omega^2 \tag{8.11}$$

$$E_{loss} = \frac{1}{2}Cv^2 \tag{8.12}$$

$$\frac{C_{pump}}{C} = \left(\frac{V}{\omega}\right)^2 = \tau_{total}^2 \tag{8.13}$$

Part IV

Conclusions

Chapter 9

Conclusions

The work starts from the analysis and modeling of an electromechanical actuation system, this system was characterized by having non-competitive performances.
Through the work of modeling and simulations some weakness have been found, to solve these, three solutions have been proposed: an electromechanical solution in which the electric motor was maintained, a high performance EMA solution (new system gear and motor) and a electro-hydraulic solution.
The realization of the Matlab&Simulink© models is followed by the design of systems and their physical realization. The comparison of the performance of prototypes has allowed a further identification of the parameters and, therefore, a detailed analysis of the intrinsic characteristics of the various technologies.
Table 9 presents the main features of the various solutions proposed and tested, in addition to their performance. These parameters show, unequivocally, what are their main advantages and disadvantages.
The EHS Maxon solution allows a very compact and lightweight construction. The performances of this system, while not being the best, are obtained with a system with the lowest rated power.
In contrast, the EMA Maxon system has the best performance at the expense of a relatively bulky construction.
The EMA Fise solution is the less efficient but it allows the re-use of the electric motor which is an advantage from the costs point of view.
At this point it is useful to outline the next steps of the project. First, it is useful to perform an experiment in the car, to better understand the performance with a real clutch and the limited spaces in the engine compartment. This condition can be useful to evaluate the thermal behavior of the solutions.
With regard to the model of the system, instead, it would be interesting to implement a second approximation of the fluid model, in which its inertial properties

will be evaluated.
In addition it may be interesting to optimize the circuit housing through a multi-physics simulation, further reducing its size and considering a future industrialization.

		EMA FISE	**EMA MAXON**	**EHS MAXON**
Electric Motor	Name	FISE Motor 12 V	Maxon RE 50 24 V	Maxon RE 40 24 V
	Max Torque [Nm]	12	8.92	2.28
	Max Speed [rpm]	500[1]	5950	7580
	Nominal Power [W]	400	200	150
	Efficiency [-]	52	94	91
	Rotor Inertia [kgm^2]	$60 \cdot 10^-6$	$54 \cdot 10^-6$	$14 \cdot 10^-6$
	Mass [g]	1200	1100	480
Transmission	Name	Maxon GP 42	Maxon GP 52	Marzocchi UK 0.5 D 1.60
	Ratio	1/12	1/4.3	-
	Displacement [cm^3/rev]	-	-	1.25
	Total Mass [kg]	2.5	2.5	1.8
	Total Volume [mm^3]	580	620	480
	Complexity	High	High	Low
Performances	Open Clutch [ms]	140	100[2] (70)	130

[1]Experimental Max Speed

[2]Obtained with $V_{in} = 70\% V_{max}$

Appendix A

Equations

A.1 Mechanical Inertia Properties

Inertial properties

The following equation refer to section 3.3.

$$\omega_{Wheel} = \omega_{DCMotor} \tag{A.1}$$

$$\omega_{Gearbox} = \tau \cdot \omega_{Wheel} \tag{A.2}$$

$$\omega_{Shaft} = \tau \cdot \omega_{Wheel} \tag{A.3}$$

$$\omega_{Cam} = \tau \cdot \omega_{Wheel} \tag{A.4}$$

$$J_{in} = J_{DCmotor} + J_{Wheel} + \frac{1}{\tau} \cdot (J_{Gearbox} + J_{Shaft} + J_{Cam}) \tag{A.5}$$

A.2 Mechanic Equations

Electro-Mechanical model equations for the State-Space modeled in section 3.8.

1° state

This state physically represents the momentum of inertia J_{in}

$$\dot{p_3} = e_1 \tag{A.6}$$

$$\dot{p_3} = -\left(K_i I_{in} + \frac{C_{in}}{J_{in}} p_3 + e_4\right) \tag{A.7}$$

$$e_4 = \tau_1 \cdot (K_f q_{11} + C_f f_9) \tag{A.8}$$

$$e_4 = \tau_1 \cdot \left(K_f q_{11} + C_f \left(\frac{\tau_1}{J_{in}} p_3 - \frac{1}{\tau_2 J_{out}} p_{13}\right)\right) \tag{A.9}$$

joining the equation (A.7) and (A.9) the result is:

$$\dot{p_3} = -\left(K_i I_{in} + \frac{C_{in}}{J_{in}} p_3 + \tau_1 \cdot \left(K_f q_{11} + C_f \left(\frac{\tau_1}{J_{in}} p_3 - \frac{1}{\tau_2 J_{out}} p_{13}\right)\right)\right) \tag{A.10}$$

rewriting the (A.10) to order the states simplifies the construction of the matrix **A**:

$$\dot{p_3} = K_i I_{in} - \frac{C_{in} + C_f \tau_1^2}{J_{in}} p_3 - \frac{K_f}{\tau} q_{11} + \frac{\tau_1 C_f}{\tau_2 J_{out}} p_{13} \tag{A.11}$$

2° state

The second state is the compressibility of the fluid in particular the variation of volume:

$$\dot{q_{11}} = f_{11} \tag{A.12}$$

$$\dot{q_{11}} = \frac{\tau_1}{J_{in}} p_3 - \frac{1}{\tau_2 J_{out}} p_{13} \tag{A.13}$$

3° state

The third state is the momentum of the mass of the clutch thrust.

$$\dot{p_{13}} = e_{13} \tag{A.14}$$

$$\dot{p_{13}} = \left(K_{out} q_{14} + \frac{C_{out}}{J_{out}} p_{13} - F_{in} - e_{12} \right) \tag{A.15}$$

$$e_{12} = \frac{1}{\tau_2} \left(K_f q_{11} + C_f \left(\frac{\tau_1}{J_{in}} p_3 - \frac{1}{\tau_2 J_{out}} p_{13} \right) \right) \tag{A.16}$$

if e_{12} (A.16) is replaced in (A.15) then

$$\dot{p_{13}} = K_{out} q_{14} + \frac{C_{out}}{J_{out}} p_{13} - F_{in} - \frac{1}{\tau_2} \left(K_f q_{11} + C_f \left(\frac{\tau_1}{J_{in}} p_3 - \frac{1}{\tau_2 J_{out}} p_{13} \right) \right) \tag{A.17}$$

rearranging the terms:

$$\dot{p_{13}} = \frac{\tau_1 C_f}{\tau_2 Jin} p_3 + \tau_1 K_f q_{11} - \frac{\left(C_{out} + \frac{C_f}{\tau_2^2} \right)}{J_{out}} p_{13} - Kout q_{14} + F_{in} \tag{A.18}$$

4° state

The fourth state is the most important in studying the behavior of the system, since it represents the slave actuator displacement, and then moving the clutch lever, this parameter is related to the change in fluid volume.

$$\dot{q_{14}} = f_{14} \tag{A.19}$$

$$\dot{q_{14}} = \frac{1}{J_{out}} p_{13} \tag{A.20}$$

A.3 Hydraulic Equations

1° State

Refer to chapter 5.2. This state represents the momentum related to the inertia J_{in}.

$$\dot{p_3} = e_1 \tag{A.21}$$

$$\dot{p_3} = -\left(K_i I_{in} + \frac{C_{in}}{J_{in}} p_3 + e_4\right) \tag{A.22}$$

$$e_4 = \tau_1 \cdot (K_f q_{11} + C_f f_9) \tag{A.23}$$

$$e_4 = \tau_1 \cdot \left(K_f q_{11} + C_f \left(\frac{\tau_1}{J_{in}} p_3 - \frac{1}{\tau_2 J_{out}} p_{13}\right)\right) \tag{A.24}$$

with equation (A.22) and (A.24):

$$\dot{p_3} = -\left(K_i I_{in} + \frac{C_{in}}{J_{in}} p_3 + \tau_1 \cdot \left(K_f q_{11} + C_f \left(\frac{\tau_1}{J_{in}} p_3 - \frac{1}{\tau_2 J_{out}} p_{13}\right)\right)\right) \tag{A.25}$$

re-writing the equation (A.26) to order the states, it simplifies the construction of the matrix **A**:

$$\dot{p_3} = K_i I_{in} - \frac{C_{in} + C_f \tau_1^2}{J_{in}} p_3 - \frac{K_f}{\tau} q_{11} + \frac{\tau_1 C_f}{\tau_2 J_{out}} p_{13} \tag{A.26}$$

2° State

The second state is the compressibility of the fluid, in particular it is the variation of the fluid volume.

$$\dot{q_{11}} = f_{11} \tag{A.27}$$

$$\dot{q_{11}} = \frac{\tau_1}{J_{in}} p_3 - \frac{1}{\tau_2 J_{out}} p_{13} \tag{A.28}$$

3° State

This state represents the mass momentum of the thrust bearing in the clutch.

$$\dot{p_{13}} = e_{13} \tag{A.29}$$

$$\dot{p_{13}} = \left(K_{out} q_{14} + \frac{C_{out}}{J_{out}} p_{13} - F_{in} - e_{12} \right) \tag{A.30}$$

$$e_{12} = \frac{1}{\tau_2} \left(K_f q_{11} + C_f \left(\frac{\tau_1}{J_{in}} p_3 - \frac{1}{\tau_2 J_{out}} p_{13} \right) \right) \tag{A.31}$$

substituting the eq. (A.31) in eq. (A.30)

$$\dot{p_{13}} = K_{out} q_{14} + \frac{C_{out}}{J_{out}} p_{13} - F_{in} - \frac{1}{\tau_2} \left(K_f q_{11} + C_f \left(\frac{\tau_1}{J_{in}} p_3 - \frac{1}{\tau_2 J_{out}} p_{13} \right) \right) \tag{A.32}$$

rearranging the terms:

$$\dot{p_{13}} = \frac{\tau_1 C_f}{\tau_2 Jin} p_3 + \tau_1 K_f q_{11} - \frac{\left(C_{out} + \frac{C_f}{\tau_2^2} \right)}{J_{out}} p_{13} - Kout q_{14} + F_{in} \tag{A.33}$$

4° State

The fourth state is the most important in studying the behavior of the system, since it represents the slave actuator displacement, and displacement of the clutch spring represents the compressibility of the fluid, in particular its variation in the fluid volume.

$$\dot{q_{14}} = f_{14} \tag{A.34}$$

$$\dot{q_{14}} = \frac{1}{J_{out}} p_{13} \tag{A.35}$$

A.4 Non Linear EMA Model

Table A.1 shows the equation the Bond-Graph model: Hydraulic fluid and clutch 8.2.

N.	Component	IN	OUT	Equation
1	S_f	e_1	f_1	$f_1 = I_{in}$
1-2	GY			$e_2 = K_i \cdot f_1 \; e_1 = K_i \cdot f_2$
3	J_{in}	e_3	f_3	$e_3 = \dot{p}_3 \; f_3 = 1/J_{in} \cdot p_3$
5	C_{in}	f_4	e_4	$e_5 = C_{in} \cdot f_5$
4-6	TF			$e_7 = 1/\tau_2 \cdot e_6 \; f_7 = \tau \cdot f_6$
7	J_{Cam}	f_7	$e_7 = \dot{p}_7$	$f_7 = p_7/J_{Cam}$
8	S_e	f_9	e_9	$e_9 = T_{Cam}$
A	**1**			$f_2 = f_3 = f_4 = f_5 \; e_2 = e_3 + e_4 + e_5$
B	**1**			$f_6 = f_7 = f_8 \; e_6 = e_7 + e_8$

Table A.1. Collection of the characteristic equation of the non linear system with Bond-Graph: Mechanical part

Table A.2 shows the equation the Bond-Graph model: Hydraulic fluid and clutch 8.4.

N.	Component	IN	OUT	Equation
1	Sf	e_1	f_1	$f_1 = v_{in}$
1-2	TF			$e_2 = 1/\tau_1 \cdot e_1 \; f_2 = \tau_1 \cdot e_1$
4	K_f	e_4	$f_4 = \dot{q}_4$	$e_4 = K_f q_4$
5	C_f	f_5	e_5	$e_5 = R \cdot f_5$
6-7	TF			$e_7 = 1/\tau_2 \cdot e_6 \; f_7 = \tau \cdot f_6$
8	m_{out}	$e_8 = \dot{p}_8$	f_8	$f_8 = p_8/m_{out}$
9	S_e	f_9	e_9	$e_9 = F_{clutch}$
10	C_{out}	f_{10}	e_{10}	$e_{10} = C_{out} \cdot f_{10}$
A	**0**			$f_2 = f_3 + f_6 \; e_2 = e_3 = e_6$
B	**1**			$e_3 = e_4 + e_5 \; f_3 = f_4 + f_5$
C	**1**			$f_7 = f_9 = f_{11} = f_{10} \; e_7 + e_9 = e_{10} + e_{11}$

Table A.2. Collection of the characteristic equation of the non linear system with Bond-Graph: hydraulic fluid and clutch

Bibliography

[1] C. Pristerà G. Romeo A. Tonoli, N. Amati. Attuazione elettroidrostatica: Modellazione e validazione sperimentale. 2009. 1.4

[2] J. A. Anderson. Variable displacement electro-hydrostatic actuator. Technical report, Dynamic controls,Inc. Dayto, 1991. 1.2

[3] Kasai H. Hattori T. Ishihara M. Uriuhara M. Asagi Y., Ogawa N. Automatic clutch control system. Patent 4591038, 1986. 1.4

[4] Zimmermann F. Werner H. Heidemeyer P., Bigalke E. Arrangement for automatic clutch actuation. Patent 4401200, 1983. 1.4

[5] http://www.bondgraph.com/. 1.5, 2.1

[6] Asano T.; Burke B.; Fox A. J. Hydraulic vehicle clutch system, drivetrain for a vehicle including same, and method. Patent, 2010. 1.4

[7] Fusi L. Sistemi di attuazione per frizioni automobilistiche., 2010. 1.5

[8] Kohlboeck M. Hydraulic system. Patent US20100155192, 2010. 1.4

[9] Caenazzo D. Mesiti D., Garabello M. An electro-device for controlling a servo-gearbox. Patent EP-802356, 1996. 1.4

[10] Kim H. S. Hwang S. H. Moon, S. E. Development of automatic clutch actuator for automated manual transmission. *International Journal of Automotive Technology*, 6(5):461–466, 2005. 1.1, 1.1, 1.4, A.4

[11] Carmine Pristerà. *Electro Hydrostatic Actuation: Industrial Applications*. PhD thesis, Politecnico di Torino, 2011. 1.3, 8.6

[12] Giuseppe Romeo. *Electro Hydrostatic Actuation: Camparison with Electro Mechanical Power Actuation Ssytem*. PhD thesis, Politecnico di Torino, 2011. 1.3, 8.6

[13] Das S. *Mechatronic modeling and simulation using bond graphs CRC*. CRC Press, 2009. 1.5, 2.1

[14] Takahashi K. Sakurai Y. Proposal of a new bond-graph method for modelling pneumatic systems. *International Journal Of Fluid Power*, (1):17–22, 2004. 1.5

[15] A.D. King S.L. Botten, C.R. Whitley. Flight control actuation technology for next-generation all-electric aircraft technology, 2000. 1.2

[16] Chan K.W. Slicker J.M. Method and apparatus for slip mode control of automatic clutch. Patent 5630773, May 1997. 1.4

[17] Jensen D. Stephen c. and David D. Flight test experience with an electromechanical actuator on the f-18 systems research aircraft. Technical report, National Aeronautics and Space Administration, 2000. 1.1, 1.4

[18] O. Wolley. *Modeling and Experimental Validation of Electro-Hydrostatic System for Automotive and Machine Tool Applications*. PhD thesis, Politecnico di Torino, 2007. 1.2, 1.4

List of Figures

1.1 Electro-Mechanical system [10] 4
1.2 Generic EHS system 5
1.3 EHA system scheme, with principal components 6
1.4 Energy losses in various EHS designs 11

3.1 Prototype SILA Holding Industriale 26
3.2 Hydraulic system model 28
3.3 Characteristic load Slave Actuator 30
3.4 BondGraph Scheme of the original sistem. 30
3.5 Slave load modeling, linear feature 34
3.6 S_e characteristic 35

4.1 Frequency response of the system (Damping neglected) 38
4.2 Mechanical equivalent of the original system 38
4.3 Simulink diagram used for simulation 42
4.4 Current trends and positions provided by SILA Holding Industriale 43
4.5 Top:Evolution in time of the slave displacement, all the damping parameters are equal to zero; Bottom: input current of the system . 44
4.6 Top: Evolution in time of the slave displacement; Bottom: input current of the system 45

4.7 Top: Evolution in time of the slave displacement, identified system; Bottom: input current of the system 45

5.1 hydraulic scheme of the system 48
5.2 Mechanical Scheme of the electro-hydraulic system 48
5.3 Bond Graph Scheme of the electro-hydrostatic system 49

6.1 Present System from SILA Holding 53
6.2 Cam 55
6.3 Modified Cam, with lower Inertia 55
6.4 Planetary gearbox example 56
6.5 Key components 57
6.6 Numerical simulation of the system with FISE motor and Maxon gearbox ($\tau = 1/12$); Opening time: 140 [ms] 58
6.7 Original Aluminum Billet 59
6.8 Support composed of four parts, easier to assemble 59
6.9 Exploded view of the whole system 59
6.10 Electromechanical System with FISE Motor 60
6.11 Numerical simulation of the system with the Maxon motor-gearbox ($\tau = 1/4.3$); Opening time: 75 [ms] 62
6.12 Electromechanical System with Maxon Motorgearbox 62
6.13 Hydraulic Scheme 64
6.14 Top: Hydraulic system performances, dotted black line is the open clutch displacement, the modeled hydraulic system opens in 70 [ms]: Bottom: Input voltage 66
6.15 Atlantic Fluid Tech: CEBP 040 NAFN, Max pressure: 350 [bar] . . 67
6.16 Atlantic Fluid Tech: COIL M7, Voltage: 12 [V], Current: 1.62 [A] . 67
6.17 Atlantic Fluid Tech: Relief Valve, Weigth: 50 [g] 68

6.18 Housing 69

6.19 Assembly Rendering 70

6.20 Imported model on Comsol 71

6.21 Model materials: Aluminum and Oil 72

6.22 Meshed model 72

6.23 Oil Pressure in the circuit 73

7.1 Test bench with the FISE electric motor 77

7.2 Linear Spring connected to the slave 78

7.3 Maxon System bottom part 78

7.4 Top: Open Clutch is set at 12 [mm], the system opens in 148 [ms] following the voltage DC; Bottom: the current has a peak near 200 [A], but the holding current is about 35 [A]. Maximum voltage: 13.5 [V] 80

7.5 Top: Open Clutch is set at 12 [mm], the system opens in 105 [ms] following the voltage DC; Bottom: the current has a peak near 60 [A], but the holding current is about 23 [A]. Maximum voltage: 13.5 [V] 81

7.6 Top: Open Clutch is set at 12 [mm], the system opens in 70 [ms] following the voltage DC; Bottom: the current has a peak near 100 [A], but the holding current is about 23 [A]. Maximum voltage: 9.5 [V] 82

7.7 Exploded view of the hydraulic system 83

7.8 Hydraulic system mounted 83

7.9 Comparison between the hydraulic and mechanical solution 84

7.10 Top: Open Clutch is set at 12 [mm], the system opens in 130 [ms] following the voltage DC; Bottom: the current has a peak a little over 40 [A], but the holding current is about 18 [A]. Maximum voltage: 13.5 [V] 85

8.1 Force acting on the cam 88
8.2 Actual displacement 88
8.3 α 88
8.4 Non linear model 88
8.5 Bond-Graph with non line cam 89
8.6 Simulink model: whole system 90
8.7 Simulink model: eccentric 91
8.8 Numeric approximation 92
8.9 Numeric approximation 93
8.10 Top: From the Duty Cycle in input (red line) the numeric response of the model in green. Bottom: Numeric Current in green and experimental in blue. 94
8.11 Numerical Current (black line) equals the experimental current . . . 95
8.12 Top: From the Duty Cycle in input (red line) the numeric response of the model in green. Bottom: Numeric Current in green and experimental in blue. 96

List of Tables

2.1 Effort and Flow in different energy domains 14

3.1 Collection of the characteristic equation of the original system with Bond-Graph 31

4.1 Equivalent model parameters 39
4.2 Comparison of natural frequencies of the two models 40
4.3 Kinectic energies 41
4.4 Modal displacements normalized to the maximum in line 41
4.5 Potential Energies 42

5.1 Equation of the bondgraph system 50

6.1 Cam Inertia (Computed using Solidworks®) 54
6.2 Motor and Gearbox Characteristics 57
6.3 Motor and Gearbox Characteristics 61
6.4 Motor and Pump Characteristics 65

8.1 Parameter identified for the FISE solution 93
8.2 Parameter identified for the high performance solution 93
8.3 Parameter identified for the hydraulic solution 95

A.1 Collection of the characteristic equation of the non linear system with Bond-Graph: Mechanical part 6

A.2 Collection of the characteristic equation of the non linear system with Bond-Graph: hydraulic fluid and clutch 6